Title	Physics of J=3/2 superconductors
Author(s)	金, 多景
Degree Grantor	北海道大学
Degree Name	博士(工学)
Dissertation Number	甲第14864号
Issue Date	2022-03-24
DOI	https://doi.org/10.14943/doctoral.k14864
Doc URL	https://hdl.handle.net/2115/85129
Type	doctoral thesis
File Information	Dakyeong_Kim.pdf

Physics of J=3/2 superconductors

Dakyeong Kim

Graduate School of Engineering
Hokkaido University
Japan
21.Feb.2022

Acknowledgement

First of all, I would like to express my sincere gratitude to my supervisor Associate Prof. Yasuhiro Asano. His guidance with immense knowledge and patience supported me in my Ph.D. study. Also, I would like to thank Prof. Kousuke Yakubo and Assistant professor. Hideaki Obuse for giving me useful advice on my research and my presentations.

I am grateful to Dr. Shingo Kobayashi for useful discussions on physics of high-spin fermions. I would like to thank Dr. T. Habe and Dr. S. Ikegaya for fruitful discussions on unconventional superconductivity.

Lastly, I would like to express my appreciation for my parents. I could finish my research on their continuous cooperation.

Contents

Chapter 1

Introduction

In 1911, superconductivity was discovered by H. K. Onnes with the disappearance of electric resistivity of Hg observed at 4.2 K.[1] After this experiment, new findings on superconductivity, such as the Meissner effect and the Josephson effect, were obtained one after another. A theoretical explanation was constructed by Bardeen, Cooper, and Schrieffer in 1957.[2] In BCS (Bardeen-Cooper-Schrieffer) theory, two electrons on the Fermi level form a Cooper pair due to an attractive interaction at a low temperature. The phase coherence of a number of Cooper pairs provides a gain in condensation energy, which stabilizes the superconducting state.

A Cooper pair has internal degree of freedom because it is a composite particle consisting of two electrons. Since an electron is an elementary particle having spin $S = 1/2$, spin of a Cooper pair is described by either spin-singlet $S = 0$ or spin-triplet $S = 1$. In addition to the spin state, the orbital part also characterize symmetry of a Cooper pair. Superconductivity in a simple metal belongs to spin-singlet s-wave symmetry class, whereas that in a high-T_c cuprates belongs to spin-singlet d-wave symmetry class. The emergence of spin-triplet superconductivity has been discussed in several Uranium compounds. Actually, the results of nuclear magnetic resonance (NMR) measurement on heavy-fermion superconductors suggested the existence of spin-triplet Cooper pairs with finite spin $S = 1$.[3, 4, 5] A group of material have attracted attention these days as various topologically nontrivial materials such as topological semimetals, topological insulators, and topological superconductors.[6, 7, 8, 9, 10, 11, 12] In most of the topological materials, more than two orbital/band overlap near the Fermi level and spin-orbit interactions modify the electronic states to be topologically nontrivial. Controlling the electromagnetic properties unique to topological materials may enable new functional devices.

Superconductivity in such a semimetal YPtBi[13, 14, 15, 16] has been considered to be topologically nontrivial. However, because of the strong spin-orbit interaction, the symmetry of the Cooper pair is very complicated. For instance, The strong coupling between spin $S = 1/2$ and orbital angular momentum $L = 1$ enables an electron with a total angular momentum $J = L + S = 3/2$. A Cooper pair in the superconducting state consists of two electrons with pseudospin $J = 3/2$. In this thesis, we refer such a superconductor as a $J = 3/2$ superconductor. The pseudospin-states of a Cooper pair can be $J = 2$ quintet and $J = 3$ septet states in addition to $J = 0$ singlet and $J = 1$ triplet states[17, 18, 19, 20]

In this thesis, we theoretically investigate physical phenomena unique to a Cooper pair with large angular momentum because only little has been known for the physics of $J = 3/2$ superconductors.[21, 22] In the thesis, we focus on pseudospin-quintet J=2 even-parity state which is a promising candidate of superconductivity in YPtBi. By solving the Bogoliubov-de Gennes (BdG) equations analytically, we will discuss the spin susceptibility, the Josephson effect, and the presence of odd-frequency Cooper pairs in J = 3/2 superconductors.

This thesis is organized as follows. In Ch. 2, we derive a microscopic model which describes the formation of $J = 3/2$ electron in the normal state. The pair potential for pseudospin-quintet even-parity states are also explained. In Ch. 3, we calculate the magnetic susceptibility of a $J = 3/2$ superconductor based on the linear response. In Ch. 4, we investigate the Josephson effect of $J = 3/2$ superconductors with paying special attention to the selection rules on Josephson current. In Ch. 5, a relation between a quasiparticle on the Bogoliubov Fermi surface (BFS) and an odd-frequency Cooper pair is discussed in a $J = 3/2$ superconductor breaking time-reversal symmetry. Finally, we summarize the overall results in Ch. 6.

Chapter 2

$J = 3/2$ Superconductor

We explain the formation of an electron with pseudospin $J = 3/2$ due to strong spin-orbit interactions and that of a Cooper pair consisting of such electrons. Luttinger and Kohn[23, 24] derived the effective Hamiltonian for an electron in a semiconductor which preserves cubic symmetry. This helps us to understand the electronic structures in a half-Heusler semimetal because the semimetal also preserves cubic symmetry. We first derive the general normal state Hamiltonian for $J = 3/2$ electrons and the pair potential for an even-parity Cooper pairing. We then derive the Bogoliubov-de Gennes (BdG) Hamiltonian by using the obtained normal state Hamiltonian and the pair potential. The anomalous Green's function is obtained by solving the Gor'kov equation analytically. The results suggest that an odd-frequency pair exists as a part of the spatial uniform ground state.

2.1 $J = 3/2$ Electrons in Semiconductors

The properties of semiconductors are qualitatively governed by the energy dispersion near the band edges. In some semiconductors such as Si with the diamond cubic structure and GaAs with the zincblende structure, the energy dispersion has a degenerate point which is protected by symmetry of crystal structure.[25] As well as the energy modulation due to spin-orbit couplings, this enriches physics of semimetals. In 1955, Luttinger derived the general Hamiltonian for an electron/hole in a semiconductor preserving cubic symmetry based on the method of invariants. Here we repeat his argument and construct the effective Hamiltonian as follows. First, we consider a semiconductor whose crystal structure belongs to T_d symmetry. Secondly, we consider an electron at a p atomic orbital which contributes to the electronic states at the band edges and has an angular momentum $l = 1$. Three conditions are necessary to derive the effective Hamiltonian,

1. The Hamiltonian is invariant under the operation of point group T_d.
2. The dispersions of an electron are quadratic function of the wavenumber.
3. The Hamiltonian is decomposed into three angular momentum matrices with $l = 1$, I_x, I_y, and I_z and their products.

Table 2.1: Character table of point group T_d.

irreps of T_d	E	$8C_3$	$3C_2$	$6S_4$	$6\sigma_d$
A_1	1	1	1	1	1
A_2	1	1	1	-1	-1
E	2	-1	2	0	0
T_1	3	0	-1	1	-1
T_2	3	0	-1	-1	1

$$I_x = \begin{pmatrix} 0 & 0 & 0 \\ 0 & 0 & -i \\ 0 & i & 0 \end{pmatrix}, \quad I_y = \begin{pmatrix} 0 & 0 & i \\ 0 & 0 & 0 \\ -i & 0 & 0 \end{pmatrix}, \quad I_z = \begin{pmatrix} 0 & -i & 0 \\ i & 0 & 0 \\ 0 & 0 & 0 \end{pmatrix}. \tag{2.1}$$

Eq. (2.1) shows the three angular momentum matrices.

From the combination of I_i matrix, nine independent terms are formed and classified to representations of T_d group as follows.

$$\begin{array}{ll} A_1 & : 1_{3\times 3} \\ E & : I_x^2 - I_y^2, I_y^2 - I_z^2 \\ T_1 & : \{I_x I_y\}, \{I_y I_z\}, \{I_z I_x\} \\ T_2 & : I_x, I_y, I_z \end{array} \tag{2.2}$$

where $\{k_i, k_j\} = (k_i k_j + k_j k_i)/2$ for cyclic i, j, k. Similarly, the quadratic terms in the component of k are classified as follows.

$$\begin{array}{ll} A_1 & : k^2 \\ E & : k_x^2 - k_y^2, k_y^2 - k_z^2 \\ T_1 & : \{k_x k_y\}, \{k_y k_z\}, \{k_z k_x\} \\ T_2 & : H_x, H_y, H_z \end{array} \tag{2.3}$$

where $H_i = (1/i)(e/c)[k_j, k_k]$. We write the character table of the point group Td in Table 2.1 and the product table of group Td in Table 2.2. From the condition 1)-3), the Hamiltonian should consist of products of the above terms and they should correspond to the representation A_1. Because the representation A_1 arises from the products of the same representation as shown in Table 2.2, the effective Hamiltonian is constructed as

$$\begin{aligned} H = {} & \alpha_1 k^2 + \alpha_2 (k_x^2 I_x^2 + k_y^2 I_y^2 + k_z^2 I_z^2) \\ & + \alpha_3 (\{k_x k_y\}\{I_x I_y\} + \{k_y k_z\}\{I_y I_z\} + \{k_z, k_x\}\{I_z I_x\}) \\ & + \alpha_4 (\boldsymbol{H} \cdot \boldsymbol{I}) \end{aligned} \tag{2.4}$$

Although the band structure changes by the material parameters α_i, the 6-fold degeneracy at the $k = 0$ point is protected by the symmetry when there is no external field (Fig. 2.1 (a)).

Spin-orbit interactions couples the spin $S = 1/2$ and the orbital angular momentum $L = 1$ of an electron. As a result, an electron is characterized by combined angular momenta $J = 3/2$ and $J = 1/2$. The combined angular momentum is referred to as a pseudospin in this thesis. In most semimetals, four-fold degenerate bands with $J = 3/2$

Table 2.2: Product table of irreps for point group T_d.

irreps of T_d	A_1	A_2	E	T_1	T_2
A_1	A_1	A_2	E	T_1	T_2
A_2	A_2	A_1	E	T_2	T_1
E	E	E	A_1+A_2+E	T_1+T_2	T_1+T_2
T_1	T_1	T_2	T_1+T_2	$A_1+E+T_1+T_2$	$A_2+E+T_1+T_2$
T_2	T_2	T_1	T_1+T_2	$A_2+E+T_1+T_2$	$A_1+E+T_1+T_2$

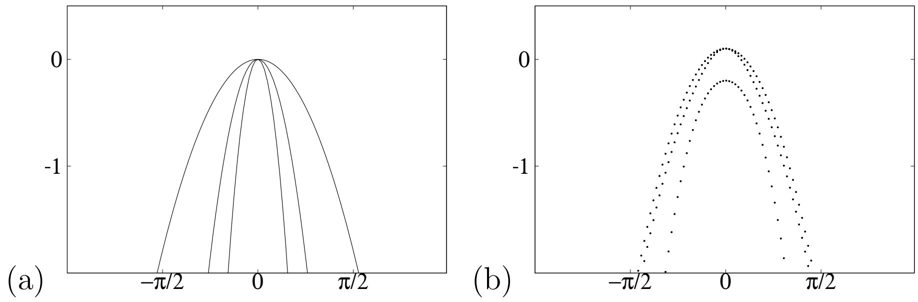

Figure 2.1: The band structure of an electron in cubic symmetry when there is no external field, (a) without spin-orbital coupling(SOC) and (b) with SOC. (a) Each bands are degenerate due to spin $\pm 1/2$. 6-fold degeneracy at $k = 0$ point is guaranteed by symmetry but specific shape depends on the material parameters. (b) Because of SOC, 6-fold band divides to 4-fold and 2-fold bands.

are dominant at the Fermi level. Thus, we neglect the effects of the two-fold degenerate bands with $J = 1/2$. The basis of the direct product space of pseudospin $J = 3/2$ can be expressed as [26]

$$\begin{aligned}
\Big|\frac{3}{2},\frac{3}{2}\Big\rangle &= \frac{1}{\sqrt{2}}\left[-\Big|p_x,\frac{1}{2}\Big\rangle - i\Big|p_y,\frac{1}{2}\Big\rangle\right] \\
\Big|\frac{3}{2},\frac{1}{2}\Big\rangle &= \frac{1}{\sqrt{6}}\left[2\Big|p_z,\frac{1}{2}\Big\rangle - \Big|p_z,-\frac{1}{2}\Big\rangle - i\Big|p_y,-\frac{1}{2}\Big\rangle\right] \\
-\Big|\frac{3}{2},\frac{1}{2}\Big\rangle &= \frac{1}{\sqrt{6}}\left[2\Big|p_z,-\frac{1}{2}\Big\rangle + \Big|p_z,\frac{1}{2}\Big\rangle - i\Big|p_y,\frac{1}{2}\Big\rangle\right] \\
-\Big|\frac{3}{2},\frac{3}{2}\Big\rangle &= \frac{1}{\sqrt{2}}\left[\Big|p_x,-\frac{1}{2}\Big\rangle - i\Big|p_y,-\frac{1}{2}\Big\rangle\right].
\end{aligned} \tag{2.5}$$

Here, we construct the effective Hamiltonian of an electron with pseudospin $J = 3/2$ in semiconductor with cubic symmetry, by using the method of invariants. In this case, the condition (3) changes and the Hamiltonian is decomposed into three 4×4 matrices with $J = 3/2$ and their products. The three matrices are given by

$$
J_1 = \frac{1}{2}\begin{pmatrix} 0 & \sqrt{3} & 0 & 0 \\ \sqrt{3} & 0 & 2 & 0 \\ 0 & 2 & 0 & \sqrt{3} \\ 0 & 0 & \sqrt{3} & 0 \end{pmatrix},
$$
$$
J_2 = \frac{i}{2}\begin{pmatrix} 0 & -\sqrt{3} & 0 & 0 \\ \sqrt{3} & 0 & -2 & 0 \\ 0 & 2 & 0 & -\sqrt{3} \\ 0 & 0 & \sqrt{3} & 0 \end{pmatrix},
$$
$$
J_3 = \frac{1}{2}\begin{pmatrix} 3 & 0 & 0 & 0 \\ 0 & 1 & 0 & 0 \\ 0 & 0 & -1 & 0 \\ 0 & 0 & 0 & -3 \end{pmatrix}. \tag{2.6}
$$

We summarize the algebra of the matrices and relations in Appendix. A. Sixteen independent matrices are generated by J_i and their products and are classified into the representations of T_d group as follows.

$$
\begin{array}{ll}
A_1 & : 1_{4\times 4} \\
A_2 & : J_x J_y J_z + J_z J_y J_x \\
E & : J_x^2 - J_y^2, J_y^2 - J_z^2 \\
T_1 & : \{J_x J_y\}, \{J_y J_z\}, \{J_z J_x\} \\
 & \quad V_x = \{(J_y^2 - J_z^2)J_x\}, V_y = \{(J_z^2 - J_x^2)J_y\}, V_z = \{(J_x^2 - J_y^2)J_z\} \\
T_2 & : J_x, J_y, J_z, \bar{J}_x = J_x^3, \bar{J}_y = J_y^3, \bar{J}_z = J_z^3
\end{array} \tag{2.7}
$$

Then the effective Hamiltonian is constructed as

$$
\begin{aligned}
\mathcal{H} =& \sum_{\boldsymbol{k}} \Psi_{\boldsymbol{k}}^\dagger \, H(\boldsymbol{k}) \, \Psi_{\boldsymbol{k}}, \\
H(\boldsymbol{k}) =& \beta_1 k^2 + \beta_2 (k_x^2 J_x^2 + k_y^2 J_y^2 + k_z^2 J_z^2) \\
&+ \beta_3 (\{k_x, k_y\}\{J_x, J_y\} + \{k_y, k_z\}\{J_y, J_z\} + \{k_z, k_x\}\{J_z, J_x\}) \\
&+ \beta_4 (H_x J_x + H_y J_y + H_z J_z) + \beta_5 (H_x \bar{J}_x + H_y \bar{J}_y + H_z \bar{J}_z), \\
\Psi_{\boldsymbol{k}} =& \left[c_{\boldsymbol{k},3/2}, c_{\boldsymbol{k},1/2}, c_{\boldsymbol{k},-1/2}, c_{\boldsymbol{k},-3/2}\right]^{\mathrm{T}},
\end{aligned} \tag{2.8}
$$

where T means the transpose of a matrix and $c_{\boldsymbol{k},j_z}$ is the annihilation operator of an electron at $\boldsymbol{k}$ with the z-component of angular momentum being j_z. We delete the elements proportional to V_i in Eq. (2.7) in the presence of time-reversal symmetry of Hamiltonian. In this thesis, we discuss resulting physical phenomena from Eq. (2.8).

2.2 $J = 3/2$ Superconductor

2.2.1 YPtBi

YPtBi is a half-Heusler compound which is supposed as a $J = 3/2$ topological superconductor. Superconductivity in YPtBi was reported at the critical temperature 0.77 K.[27]

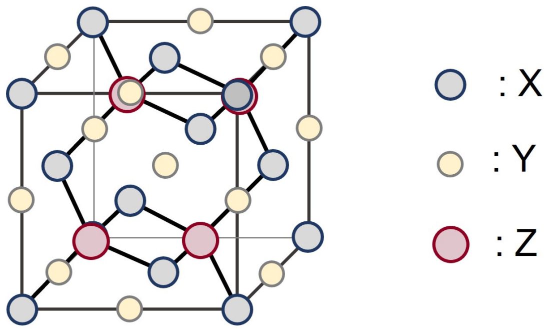

Figure 2.2: The crystal structure of half-Heusler semimetals.

Half-Heusler compound is a ternary compound consisting of three different atoms (X, Y, and Z), where X and Y are transition metals and Z is a p-block element. It has a cubic structure classified to T_d symmetry while inversion symmetry is broken (Fig. 2.2). Strong SOC is realized when Z is an heavy atom like Bi.[28] As well as YPtBi, half-Heusler compounds such as LaPtBi or LuPtBi are also proposed to be topologically nontrivial material.[29, 30, 31, 32]

In the presence of the SOC, the four-fold degenerate bands appear near the Fermi level in semimetals, which are similar to those of a semiconductor preserving cubic symmetry as shown in the left panel in Fig. 2.3. It is the band inversion that makes YPtBi fundamentally different from usual semiconductors. In the presence of strong SOC, the energy at bottom of $s_{1/2}(\Gamma_6)$ bands becomes lower than that at the top of the $p_{3/2}(\Gamma_8)$ bands as shown in the right panel in Fig. 2.3.[28] As a result, the $p_{3/2}(\Gamma_8)$ bands split into two two-fold degenerate bands which are characterized by $J = \pm 3/2$ and $J = \pm 1/2$. One band goes upward and the other goes downward as shown in Fig. 2.3. The four-fold degeneracy at Γ point remains in the presence of cubic symmetry. For YPtBi, the band inversion has been observed by angular-resolved-photoemission spectroscopy (ARPES).[26] When YPtBi undergoes the transition to superconducting phase at a low temperature, two electrons with $J = 3/2$ form a Cooper pair.

2.2.2 Bogoliubov-de Gennes Hamiltonian

We explain the Bogoliubov-de Gennes (BdG) Hamiltonian which we analyze in this thesis. We consider even-parity pseudospin J = 3/2 superconductors which preserve cubic symmetry. We are thinking that YPtBi corresponds to a specific case of such a material although inversion symmetry is broken in YPtBi. This assumption is justified because effects of breaking inversion symmetry on the band structure are totally negligible.[15]

The Bogoliubov–de Gennes(BdG) Hamiltonian is expressed in terms of the normal Hamiltonian H_N and the pair potential $H_\Delta(\boldsymbol{k})$ as

$$H_{\rm BdG}(\boldsymbol{k}) = \begin{bmatrix} H_{\rm N}(\boldsymbol{k}) & H_\Delta(\boldsymbol{k}) \\ -\underset{\sim}{H_\Delta}(\boldsymbol{k}) & -\underset{\sim}{H}_{\rm N}(\boldsymbol{k}) \end{bmatrix}, \tag{2.9}$$

where $\underset{\sim}{X}(\boldsymbol{k}, i\omega) \equiv X^*(-\boldsymbol{k}, i\omega)$ represents the particle-hole conjugation of $X(\boldsymbol{k}, i\omega)$. Because of the high pseudospin of quasiparicles, the dimension of the state space is higher than that of usual spin $S = 1/2$ electron. Therefore, the BdG Hamiltonian is expressed

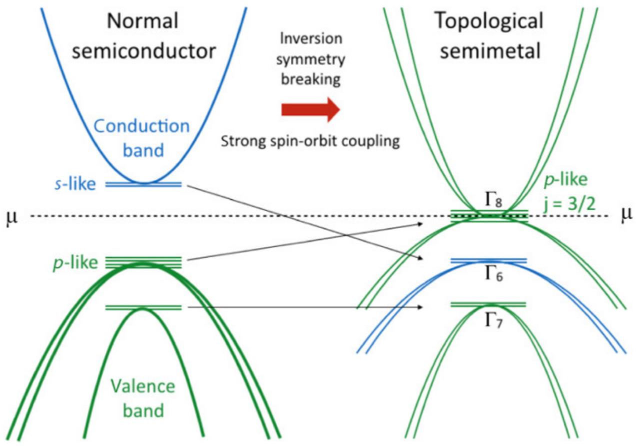

Figure 2.3: The schematic figure which describes band inversion.[26] The left figure shows the s-like conduction band and the p-like valence band of a normal semiconductor. When SOC is strong enough, both bands mix and result in the right figure which shows pseudospin $J = 3/2$ conduction band with four-fold degenerate point near the Fermi level.

as an 8×8 matrix while it is a 4×4 matrix for usual spin $S = 1/2$ superconductor. The BdG Hamiltonian preserves particle-hole symmetry,

$$\mathcal{C} H_{\mathrm{BdG}}(-\boldsymbol{k})\mathcal{C}^{-1} = -H_{\mathrm{BdG}}(\boldsymbol{k}), \quad \mathcal{C} = \tau_1 \mathcal{K}, \tag{2.10}$$

where τ_i for $i = 1 - 3$ is the Pauli matrix in particle-hole space.

Normal Hamiltonian

We can adopt the general Hamiltonian in Eq. (2.8) as the normal state Hamiltonian. In absence of external magnetic field, the Hamiltonian is rewritten as

$$H_N(\boldsymbol{k}) = a_1 \boldsymbol{k}^2 + 2a_2 \sum_i k_i^2 J_i^2 + a_3 \sum_{i \neq j} k_i k_j J_i J_j - \mu. \tag{2.11}$$

The material parameters a_i for YPtBi have been reported.[30, 26] The Hamiltonian in Eq. (2.11) also can be transformed into terms in the γ matrices,

$$H_N(\boldsymbol{k}) = \varepsilon_0(\boldsymbol{k}) + \sum_{\nu=1}^{5} \varepsilon_\nu(\boldsymbol{k})\gamma^\nu - \mu = \mathbb{E}_{\boldsymbol{k}}, \tag{2.12}$$

with coefficients,

$$\varepsilon_0(\boldsymbol{k}) = \frac{|\boldsymbol{k}|^2}{2m_0}, \quad \varepsilon_{j=1-3}(\boldsymbol{k}) = \frac{|\boldsymbol{k}|^2}{2m_1} e_{j=1-3}(\hat{\boldsymbol{k}}), \quad \varepsilon_{j=4,5}(\boldsymbol{k}) = \frac{|\boldsymbol{k}|^2}{2m_2} e_{j=4,5}(\hat{\boldsymbol{k}}),$$
$$m_0 = \frac{1}{2}\left(a_1 + \frac{5}{4}a_2\right)^{-1}, \quad m_1 = \frac{1}{a_3}, \quad m_2 = \frac{1}{2a_2}, \tag{2.13}$$

where $\boldsymbol{\varepsilon}(\boldsymbol{k})$ is a five-component vector. The definition and algebras of the γ matrices are presented in Appendix. A. The functions $e_\nu(\hat{\boldsymbol{k}})$ are defined by

$$e_1(\hat{\boldsymbol{k}}) = \sqrt{3}\hat{k}_x\hat{k}_y, \quad e_2(\hat{\boldsymbol{k}}) = \sqrt{3}\hat{k}_y\hat{k}_z, \quad e_3(\hat{\boldsymbol{k}}) = \sqrt{3}\hat{k}_z\hat{k}_x,$$
$$e_4(\hat{\boldsymbol{k}}) = \frac{\sqrt{3}}{2}(\hat{k}_x^2 - \hat{k}_y^2), \quad e_5(\hat{\boldsymbol{k}}) = \frac{1}{2}(2\hat{k}_z^2 - \hat{k}_x^2 - \hat{k}_y^2), \tag{2.14}$$

where $\hat{k}_i = k_i/|\boldsymbol{k}|$ and normalized, *i.e.* $\sum_{\nu=1}^{5} e_\nu^2(\hat{\boldsymbol{k}}) = 1$. Since $|m_0| \geq \sqrt{6}\,|m_1|$ is satisfied in YPbBi, two bands curve upwards and the remaining two bands curve downwards.[15]

The Hamiltonian in Eq. (2.12) poses time-reversal symmetry (TRS),

$$\mathcal{T} H_N(-\boldsymbol{k})\mathcal{T}^{-1} = H_N(\boldsymbol{k}), \tag{2.15}$$

$$\mathcal{T} = U_T\mathcal{K}, \quad U_T = \gamma^1\gamma^2, \tag{2.16}$$

where U_T is the unitary part of time-reversal operation with $\mathcal{K}$ meaning complex conjugation. Under the time-reversal operation, γ^ν and J_i show the relation,

$$\mathcal{T}\,\gamma^\nu\,\mathcal{T}^{-1} = -U_T\,(\gamma^\nu)^*\,U_T = \gamma^\nu, \quad \nu = 0-5, \tag{2.17}$$

$$\mathcal{T}\,J_i\,\mathcal{T}^{-1} = -U_T\,(J_i)^*\,U_T = -J_i, \quad i = 1-3. \tag{2.18}$$

The matrix γ^ν remains unchanged, whereas J_i changes its sign.

Pair potential

In the BCS (Bardeen–Cooper–Schrieffer) theory, superconductivity occurs because a pair of two electrons are bound by attractive interactions between them and a number of such electron pairs condense coherently. The superconducting order parameter called pair potential,

$$\Delta_{\alpha,\beta} = \frac{1}{V_{\mathrm{vol}}}\sum_{\boldsymbol{p}} g(\boldsymbol{k}-\boldsymbol{p})\langle c_{\boldsymbol{p},\alpha}c_{-\boldsymbol{p},\beta}\rangle \tag{2.19}$$

where $c_{\boldsymbol{p},\alpha}$ is an annihilation operator of an electron, $\alpha(\beta)$ refers spin of an electron, and g denotes the attractive interaction between two electrons. $\langle c_{\boldsymbol{p},\alpha}c_{-\boldsymbol{p},\beta}\rangle$ is called pairing correlation. The pair potential is defined as a product of the pairing correlation and the attractive interaction supporting it. The pair potential is represented as a matrix in spin of a Cooper pair.

The pairing correlation can be classified in terms of symmetry of the pairing correlation under the permutation of two electrons. For conventional $S = 1/2$ superconductors, the pairing correlations are classified into four classes as shown in Table2.3. The pairing of two spin $S = 1/2$ electrons results in a $S = 0$ spin-singlet or $S = 1$ spin-triplet state. Because electrons are fermions and obey the Fermi-Dirac statistics, the pairing state of two electrons must be antisymmetric under the permutation of two electrons. In a $J = 3/2$ superconductor, two electrons with pseudospin $J = 3/2$ form a Cooper pair. In addition to $J = 0$ singlet and $J = 1$ triplet states, pseudospin of a Cooper pair can be $J = 2$ quintet and $J = 3$ septet states as shown in Table 2.4. In this thesis, we discuss how high-angular momentum of Cooper pairs affect physics of $J = 3/2$ superconductors.

In this thesis, we focus on an even-parity superconductor with time-reversal symmetry (TRS). The pair potential has a general form[33]

$$H_\Delta(\boldsymbol{k}) = \eta_{\boldsymbol{k},0}U_T + \boldsymbol{\eta}_{\boldsymbol{k}}\cdot\boldsymbol{\gamma}U_T. \tag{2.20}$$

The first term refers to the pair potential of pseudospin-singlet state and the second term refers to that of pseudospin-quintet state. The amplitudes $\eta_{\boldsymbol{k},0}$ and a five-component

Table 2.3: Classification of Cooper pairs consisting of two $S = 1/2$ electrons according to the symmetries under permutation. The frequency refers the Matsubara frequency.

Pairing	Frequency	Spin	Parity
ESE	even	singlet	even
ETO	even	triplet	odd
OTE	odd	triplet	even
OSO	odd	singlet	odd

Table 2.4: Classification of Cooper pairs consisting of two $J = 3/2$ quasiparticles according to symmetries under permutation. The singlet and quintet state are even under the permutation and triplet and septet state are odd.

frequency	pseudo-spin	parity
even	singlet	even
	quintet	even
	triplet	odd
	septet	odd
odd	triplet	even
	septet	even
	singlet	odd
	quintet	odd

vector $\boldsymbol{\eta_k}$ are even in momentum and real in the presence of TRS. It is easy to confirm that Eq. (2.20) preserves time-reversal symmetry,

$$\mathcal{T}\, H_\Delta(\boldsymbol{k})\, \mathcal{T}^{-1} = H_\Delta(\boldsymbol{k}), \tag{2.21}$$

by using Eq. (2.17). Because electrons obey the Fermi-Dirac statistics, the pair potential must be antisymmetric under the permutation of two electrons forming a Cooper pair,

$$H_\Delta^{\mathrm{T}}(-\boldsymbol{k}) = -H_\Delta(\boldsymbol{k}), \tag{2.22}$$

where the permutation of pseudospin is carried out by taking the transpose of the matrix (T).

When we also assume cubic symmetry of a superconductor, possible pair potentials and pairing states are restricted to which can be decomposed to irreducible representations(irreps) of the cubic symmetry. We list the irreps of the point group O_h and their basis as shown in Table 2.5. For even-parity s-wave quintet state, the pair potential corresponding to the E_g or T_{2g} irreps become

$$\begin{aligned} \mathrm{E}_g : H_\Delta(\boldsymbol{k}) &= \Delta(h_{3z^2-r^2}\Gamma_{3z^2-r^2} + h_{x^2-y^2}\Gamma_{x^2-y^2}) \\ &= \Delta(h_{3z^2-r^2}\gamma^5 + h_{x^2-y^2}\gamma^4)\, U_T, \end{aligned} \tag{2.23}$$

$$\begin{aligned} \mathrm{T}_{2g} : H_\Delta(\boldsymbol{k}) &= \Delta(l_{yz}\Gamma_{yz} + l_{zx}\Gamma_{zx} + l_{xy}\Gamma_{xy}) \\ &= \Delta(l_{yz}\gamma^2 + l_{zx}\gamma^3 + l_{xy}\gamma^1)\, U_T, \end{aligned} \tag{2.24}$$

where each pair potential is characterized by the vectors $\boldsymbol{h} = (h_{3z^2-r^2}, h_{x^2-y^2})$ or $\boldsymbol{l} = (l_{yz}, l_{zx}, l_{xy})$. We list the possible values for the vectors $\boldsymbol{h}$ and $\boldsymbol{l}$ in Table 2.6.[33]

Table 2.5: Possible pairing states in a $J = 3/2$ cubic superconductors, which are decomposed into the basis of irreducible representations (irreps) of cubic symmetric point group O_h. Here, $1_{4\times4} \times U_T$ corresponds to a basis of singlet state, $(\mathcal{J}_1, \mathcal{J}_2, \mathcal{J}_3)$ to triplet states, $(\Gamma_{yz}, \Gamma_{zx}, \Gamma_{xy}, \Gamma_{x^2-y^2}, \Gamma_{3z^2-r^2})$ to quintet states, and $(W_1, W_2, W_3, W_4, W_5, W_6, W_7)$ to septet states, respectively.

irrep of O_h	basis	pairing
A_{1g}	$1_{4\times4} \times U_T$	singlet
A_{2g}	$W_7 = 1/\sqrt{3}(J_xJ_yJ_z + J_zJ_yJ_x) \times U_T$	septet
E_g	$(\Gamma_{x^2-y^2}, \Gamma_{3z^2-r^2}) = \left[1/\sqrt{3}(J_x^2 - J_y^2), 1/3(2J_z^2 - J_x^2 - J_y^2)\right] \times U_T$	quintet
T_{1g}	$(\mathcal{J}_1, \mathcal{J}_2, \mathcal{J}_3) = \left(2/\sqrt{5}J_x, 2/\sqrt{5}J_y, 2/\sqrt{5}J_z\right) \times U_T$	triplet
	(W_1, W_2, W_3)	septet
	$= 2\sqrt{5}/3\left[\left(J_x^3 - 41/20J_x\right), \left(J_y^3 - 41/20J_y\right), \left(J_z^3 - 41/20J_z\right)\right] \times U_T$	
T_{2g}	$(\Gamma_{yz}, \Gamma_{zx}, \Gamma_{xy})$	quintet
	$= 1/\sqrt{3}\left[\left(J_yJ_z + J_zJ_y\right), \left(J_zJ_x + J_xJ_z\right), \left(J_xJ_y + J_yJ_x\right)\right] \times U_T$	
	(W_4, W_5, W_6)	septet
	$= 1/\sqrt{3}\left[\left\{J_x, (J_y^2 - J_z^2)\right\}, \left\{J_y, (J_z^2 - J_x^2)\right\}, \left\{J_z, (J_x^2 - J_y^2)\right\}\right] \times U_T$	

Table 2.6: The ordering vectors which describe possible pair potentials for even-parity s-wave superconductors given by a Landau analysis.[33]

irrep of O_h	TRS	TRSB
E_g	$(1,0), (0,1)$	$(\pm i, 1)$
T_{2g}	$(1,0,0), (1,1,1)$	$(1, \pm i, 0), (0, 1, \pm i), (\pm i, 0, 1)$ $(1, \omega^{\pm1}, \omega^{\mp1}), (1, \omega^{\pm1}, \omega^{\pm2}), (1, \omega^{\pm2}, \omega^{\pm1}), (1, \omega^{\pm2}, \omega^{\mp2})$

2.3 Pairing states

Although a superconducting state is characterized by a pair potential belonging to a symmetry class in Table 2.4, there exist a Cooper pair that belongs to different symmetry classes from the symmetry of the pair potential. In this section, we introduce the anomalous Green's function which refers correlation function of Cooper pairs.

2.3.1 Green's function

The Matsubara Green's function is a correlation function of two annihilation/creation operators defined by

$$\{G(\boldsymbol{k}, i\omega_n)\}_{\alpha\beta} = -\int_0^{1/T} d\tau \left\langle T_\tau c_{\boldsymbol{k},\alpha}(\tau) c^\dagger_{\boldsymbol{k},\beta} \right\rangle e^{i\omega_n\tau}, \tag{2.25}$$

$$\{F(\boldsymbol{k}, i\omega_n)\}_{\alpha\beta} = -\int_0^{1/T} d\tau \left\langle T_\tau c_{\boldsymbol{k},\alpha}(\tau) c_{\boldsymbol{k},\beta} \right\rangle e^{i\omega_n\tau}. \tag{2.26}$$

In the mean-field theory of superconductivity, a quasiparticle and a Cooper pair are described by the normal Green's function $G(\boldsymbol{k}, i\omega_n)$ and the anomalous Green's function

$F(\boldsymbol{k}, i\omega_n)$, respectively. Therefore, the anomalous Green's function is zero in the normal state.

The Green's function for a superconducting state can be obtained by solving the Gor'kov equation,

$$\Big[i\omega_n - H_{\rm BdG}(\boldsymbol{k})\Big] \begin{bmatrix} G(\boldsymbol{k}, i\omega_n) & F(\boldsymbol{k}, i\omega_n) \\ -\underset{\sim}{F}(\boldsymbol{k}, i\omega_n) & -\underset{\sim}{G}(\boldsymbol{k}, i\omega_n) \end{bmatrix} = 1_{8\times 8}. \tag{2.27}$$

By substituting the BdG Hamiltonian in Eq. (2.9), each Green's function is calculated as

$$\begin{aligned} G(\boldsymbol{k}, i\omega_n) &= \Big[(i\omega_n - H_{\rm N}) + H_\Delta (i\omega_n + \underset{\sim}{H}_{\rm N})^{-1} \underset{\sim}{H_\Delta}\Big]^{-1}, \\ F(\boldsymbol{k}, i\omega_n) &= \Big[\underset{\sim}{H_\Delta} + (i\omega_n + \underset{\sim}{H}_{\rm N}) H_\Delta^{-1} (i\omega_n - H_{\rm N})\Big]^{-1}. \end{aligned} \tag{2.28}$$

It is clear that for the normal state, *i.e.*, $H_\Delta = 0$, the anomalous Green's function is zero. When the dispersion relation is independent of the pseudospin, *i.e.* $H_N(\boldsymbol{k}) = (\varepsilon_0(\boldsymbol{k}) - \mu)\gamma^0 = \xi_{\boldsymbol{k}}\gamma^0$, Eq. (2.28) is simplified to

$$\begin{aligned} G(\boldsymbol{k}, i\omega_n) &= [H_\Delta \underset{\sim}{H_\Delta} - (\omega_n^2 + \xi_{\boldsymbol{k}}^2)]^{-1} (i\omega_n + \xi_{\boldsymbol{k}})\gamma^0, \\ F(\boldsymbol{k}, i\omega_n) &= [H_\Delta \underset{\sim}{H_\Delta} - (\omega_n^2 + \xi_{\boldsymbol{k}}^2)]^{-1} H_\Delta. \end{aligned} \tag{2.29}$$

2.3.2 Odd-frequency Pairing

The pairing correlation function is defined by

$$f_{\alpha,\beta}(\boldsymbol{k}, \tau - \tau') = -\left\langle T_\tau c_\alpha(\boldsymbol{k}, \tau)\, c_\alpha(\boldsymbol{k}, \tau')\right\rangle, \tag{2.30}$$

where τ is imaginary time. Therefore, the correlation function Fourier transformed in τ is represented by the anomalous Green's function in Eq. (2.28) so that we can investigate pairing states in a superconductor by analyzing it. We find that $[H_N, H_\Delta] \neq 0$ is required to have finite odd-frequency correlation function, *i.e.*, odd-frequency pair exists. An odd-frequency pair is a Cooper pair with odd-frequency symmetry, such as a pair belonging to OTE or OSE class for $S = 1/2$ superconductors in Table 2.3. In 2016, A. Ramires, and M. Sigrist proposed the concept of superconducting fitness, which quantifies the incompatibility between the gap and the band structure.[34] The fitness $f(\boldsymbol{k})$ is defined as

$$\begin{aligned} [H_N(\boldsymbol{k}), H_\Delta(\boldsymbol{k})]^* &= H_N(\boldsymbol{k}) H_\Delta(\boldsymbol{k}) - H_\Delta(\boldsymbol{k}) H_N^*(-\boldsymbol{k}) \\ &= f(\boldsymbol{k})(i\sigma_2). \end{aligned} \tag{2.31}$$

The authors linked the quantity of fitness to the suppression of the superconducting critical temperature in a symmetry-breaking field. In an even-parity superconductor, it is easy to confirm that finite fitness corresponds to the condition for the appearance of an odd-frequency pair. Thus we can infer that the suppression of the critical temperature is the effect of an odd-frequency pairing. Like this, odd-frequency pair tends to show physics opposite to that of even-frequency pair.

In Fig. 2.4, we present places where an odd-frequency Cooper pair exists. In the case of single-band, an odd-frequency Cooper pair appears as a subdominant pairing correlation that localizes various places such as a vortex core, a surface, and a junction interface to another material. The odd-frequency pairing correlations in these cases describe the local deformation of the superconducting condensate [35]. A spin-triplet s-wave Cooper pair generated by the exchange potential in a ferromagnet [36] is the most well-known example of an odd-frequency pair. The exchange potential polarizes and flips the spin of an electron, which causes the symmetry conversion between spin-singlet and spin-triplet. At a surface of an unconventional superconductor, Andreev bound states appear due to the sign change of the pair potential. The surface breaks inversion symmetry locally and generates an odd (even)-parity Cooper pair from an even (odd)-parity pair in the bulk [37, 35]. Majorana fermion which is a quasiparticle at a specialized Andreev bound state also accompanies an odd-frequency pair.[38] As far as we know, an odd-frequency pair exhibits paramagnetic response to an external magnetic field.[39, 40, 41] A usual (even-frequency) Cooper pair is diamagnetic and excludes magnetic fields. Therefore, a superconductor can maintain its macroscopic phase being uniform in real space and can decrease the condensation energy. A paramagnetic Cooper pair, on the other hand, is unstable thermodynamically because it causes spatial variations in the superconducting phase.[42, 43, 44] Thus the appearance of an odd-frequency pair drastically modifies local magnetic properties such as the surface impedance of a junction [40] and the magnetic susceptibility of a small unconventional superconductor.[44]

In contrast to single-band superconductors, the odd-frequency pairing correlation exists as a part of the uniform ground state [45] in a multi-orbital/band superconductors, as shown in Fig. 2.4(b). The existence of an odd-frequency pair in a uniform superconductor was pointed out in a multiband superconductor, where the band hybridization generates an odd-frequency Cooper pair.[45] However, the nature of an odd-frequency pair in the bulk is not yet well understood with following exceptions. An odd-frequency pair suppresses T_c [41] because it decreases the pair density and the condensation energy. Odd-frequency pairs induced in the bulk are known to stabilize the Josephson π-state.[46, 47]

For an even-parity $J = 3/2$ superconductor, pseudospin-triplet/septet pair is expected to appear as the pairing correlations belonging to the odd-frequency symmetry class. Here, we note the anomalous Green's function for a $J = 3/2$ superconductor with pseudospin-dependent normal Hamiltonian and pseudospin-quintet pair potential as an example case with $[H_N, H_\Delta] \neq 0$,

$$H_N = \xi_{\boldsymbol{k}}\gamma^0 + \boldsymbol{\varepsilon}_{\boldsymbol{k}} \cdot \boldsymbol{\gamma} \tag{2.32}$$

$$H_\Delta = (\boldsymbol{\eta}_{\boldsymbol{k}} \cdot \boldsymbol{\gamma})U_T. \tag{2.33}$$

It is calculated as

$$\begin{aligned} F(\boldsymbol{k}, i\omega_n) = \Big[& U_T(\boldsymbol{\eta}_{\boldsymbol{k}} \cdot \boldsymbol{\gamma}) + \frac{1}{|\boldsymbol{\eta}|} U_T \left\{ \omega_n^2 + (\xi_{-\boldsymbol{k}}\gamma^0 + \boldsymbol{\varepsilon}_{\boldsymbol{k}} \cdot \boldsymbol{\gamma})^2 \right\} (\boldsymbol{\eta}_{\boldsymbol{k}} \cdot \boldsymbol{\gamma}) \\ & + \frac{1}{|\boldsymbol{\eta}|} U_T \left(i\omega_n + \xi_{-\boldsymbol{k}}\gamma^0 + \boldsymbol{\varepsilon}_{-\boldsymbol{k}} \cdot \boldsymbol{\gamma} \right) [\boldsymbol{\eta}_{\boldsymbol{k}} \cdot \boldsymbol{\gamma}, \boldsymbol{\varepsilon}_{\boldsymbol{k}} \cdot \boldsymbol{\gamma}] \Big]^{-1}. \end{aligned} \tag{2.34}$$

The odd-frequency term is proportional to the commutation term, $[\boldsymbol{\eta}_{\boldsymbol{k}} \cdot \boldsymbol{\gamma}, \boldsymbol{\varepsilon}_{\boldsymbol{k}} \cdot \boldsymbol{\gamma}]$.

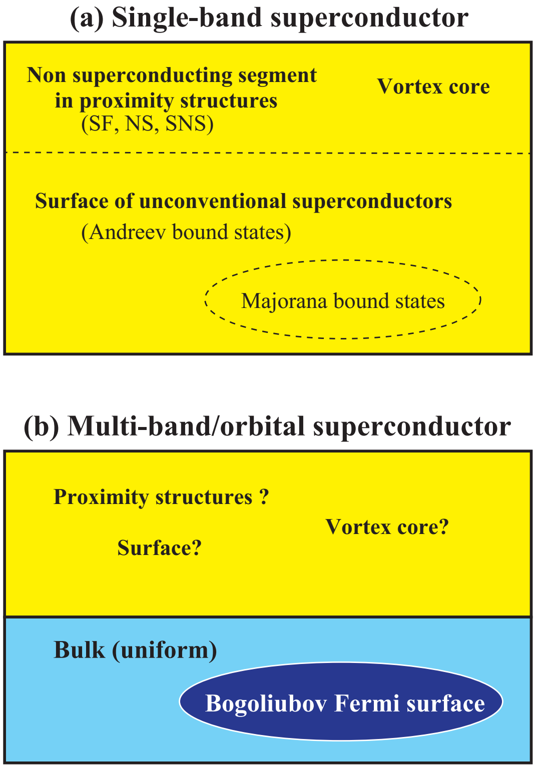

Figure 2.4: Places where an odd-frequency Cooper pair exists (a) in a single-band superconductor and (b) in a two-band/orbital superconductor. (a) Spatially uniform odd-frequency pairing correlations are absent in a single-band superconductor. Therefore, an odd-frequency pair exists as the subdominant correlations which spatially localize (b) In two-band/orbital superconductors, an odd-frequency pair exists as a spatially uniform subdominant pairing correlation in the bulk as well as a local deformation of the condensate. A quasiparticle on the BFS appears due to extra degrees of freedom in the electronic structure in the absence of time-reversal symmetry (will be discussed in Ch. 5).[17] The physical phenomena caused by an odd-frequency pair in the bulk have been an open issue.

Chapter 3

Magnetic Susceptibility

3.1 Introduction

In 1998, the results of nuclear magnetic resonance (NMR) measurement on UP_3 was reported which showed spin susceptibility independent of the temperature.[3] This made reliable the argument that UP_3 is a spin-triplet superconductor. Besides, the NMR measurement has been used to investigate spin-triplet superconductors with unconventional spin-state.[4, 5] However, Frigeri *et al* showed that spin susceptibility of a spin-singlet superconductor approaches to that of a spin-triplet superconductor, in the presence of spin-orbit coupling (SOC).[48] Therefore, we expect that SOC, the origin of pseudospin, also affects magnetic behaviors of $J = 3/2$ superconductors.

In this chapter, we investigate magnetic susceptibility of $J = 3/2$ superconductors. We begin with the linear response theory for calculating magnetic susceptibility by using the Green's function. We first calculate the spin susceptibility in $S = 1/2$ superconductors and discuss effects of SOC on the results. Then we show the magnetic susceptibility in $J = 3/2$ superconductors and compare the obtained results with those in $S = 1/2$ superconductors.

3.2 Spin Susceptibility in $S = 1/2$ Superconductors

The magnetic moment in a $S = 1/2$ superconductor is defined by

$$\boldsymbol{m}(\boldsymbol{r}) = \frac{g\mu_B}{2}\sum_{\alpha,\beta}\psi^\dagger_\alpha(\boldsymbol{r})\boldsymbol{\sigma}_{\alpha,\beta}\psi_\beta(\boldsymbol{r}), \tag{3.1}$$

where $\psi_{\lambda,\alpha}(\boldsymbol{r})$ is annihilation operator of an electron, and α, β is for spin of the electron. Within the linear response, the magnetic moment at the time t is calculated in a time-dependent Zeeman field $H(\mathrm{x})$ as follows (Appendix. B),

$$m_i(\mathrm{x}) = \frac{i}{\hbar}\int_{-\infty}^{t} dt' \int d\boldsymbol{r}' \langle [m_i(\mathrm{x}), m_j(\mathrm{x}')]\rangle H_j(\mathrm{x}'), \tag{3.2}$$

where $\mathrm{x} = (t, \boldsymbol{r})$. The equation is rewritten by using the retarded correlation function $Q_{ij}(\mathrm{x}, \mathrm{x}')$,

$$m_i(\mathrm{x}) = -\frac{1}{\hbar}\int d\mathrm{x}' Q_{ij}(\mathrm{x}, \mathrm{x}') H_j(\mathrm{x}') \tag{3.3}$$

$$Q_{ij} = -i\theta(t-t')\langle [m_i(\mathrm{x}), m_j(\mathrm{x}')]\rangle. \tag{3.4}$$

The retarded correlation function is represented in terms of the Green's function.

$$Q_{ij}(\mathrm{x}, \mathrm{x}') = -\left(\frac{g\mu_B}{2}\right)^2 \sum_{\alpha,\beta}\sum_{\alpha',\beta'} \sigma^i_{\alpha,\beta}\sigma^j_{\alpha',\beta'} \times \ \langle T_\tau \psi^\dagger_\alpha(\mathrm{x})\psi_\beta(\mathrm{x})\psi^\dagger_{\alpha'}(\mathrm{x}')\psi_{\beta'}(\mathrm{x}')\rangle \tag{3.5}$$

$$\begin{aligned} &= -\left(\frac{g\mu_B}{2}\right)^2 \sum_{\alpha,\beta}\sum_{\alpha',\beta'} \sigma^i_{\alpha,\beta}\sigma^j_{\alpha',\beta'} \\ &\times \left[-G_{\beta'\alpha}(\mathrm{x}'-\mathrm{x})G_{\beta,\alpha'}(\mathrm{x}-\mathrm{x}') - \underset{\sim}{F}_{\alpha',\alpha}(\mathrm{x}'-\mathrm{x})F_{\beta,\beta'}(\mathrm{x}-\mathrm{x}')\right]. \end{aligned} \tag{3.6}$$

In a uniform superconductor, the Fourier component is represented by

$$\begin{aligned} &Q_{ij}(\boldsymbol{q}, i\omega_n) \\ &= \left(\frac{g\mu_B}{2}\right)^2 \frac{k_B T}{\hbar}\sum_{\omega_l}\int \frac{d\boldsymbol{k}}{(2\pi)^d} \\ &\times \mathrm{Tr}\ \left[G(\boldsymbol{k}_-, i\omega_l)\sigma^\mu G(\boldsymbol{k}_+, i\omega_l + i\omega_n)\sigma^\nu + \underset{\sim}{F}(\boldsymbol{k}_-, i\omega_l)\sigma^\mu F(\boldsymbol{k}_+, i\omega_l + i\omega_n)(\sigma^\nu)^T\right] \end{aligned} \tag{3.7}$$

where $\boldsymbol{k}_\pm = \boldsymbol{k} \pm \boldsymbol{q}/2$. Spin susceptibility is calculated as

$$\chi_{ij}(\boldsymbol{q}, \omega) = -\frac{1}{\hbar} Q_{ij}(\boldsymbol{q}, i\omega_n \to \omega + i\delta). \tag{3.8}$$

Finally, we take the limit $\boldsymbol{q} \to 0$ and $i\omega_n \to \omega + i\delta \to 0$ as a Zeeman field is uniform in space and static in time.

In this section, we assume the normal Hamiltonian

$$H_N(\boldsymbol{k}) = \xi_{\boldsymbol{k}} + (\boldsymbol{\lambda}\times\boldsymbol{k})\cdot\boldsymbol{\sigma} = \xi_{\boldsymbol{k}} + \boldsymbol{L}_{\boldsymbol{k}}\cdot\boldsymbol{\sigma}, \tag{3.9}$$

where the last term refers to the Hamiltonian due to the spin-orbit coupling and $\boldsymbol{\lambda}$ represents the lack of inversion symmetry. Trivially, $\boldsymbol{L}_{-\boldsymbol{k}} = -\boldsymbol{L}_{\boldsymbol{k}}$. The broken symmetry yields a coupling between spin-singlet and triplet channel, but we can ignore it in the limit of $\langle|\boldsymbol{L}_{\boldsymbol{k}}|\rangle_{\boldsymbol{k}} \ll \varepsilon_{\boldsymbol{k}}$.[48] Therefore, we discuss spin-singlet state and spin-triplet state separately. The Green's functions to calculate Eq. (3.7) are achieved from the Gor'kov equation in Eq. (2.28).

3.2.1 Normal state

At a temperature above the critical temperature, a material is in the normal state. The pair potential and the anomalous Green's function is zero. The Green's function of the normal state for a $S = 1/2$ superconductor is given by

$$G(\boldsymbol{k}, i\omega_n) = \frac{1}{(i\omega_n - \xi_k)^2 - |\boldsymbol{L}_{\boldsymbol{k}}|^2}\left(i\omega_n - \xi_k\sigma_0 + \boldsymbol{L}_{\boldsymbol{k}}\cdot\boldsymbol{\sigma}\right), \tag{3.10}$$

$$F(\boldsymbol{k}, i\omega_l) = 0. \tag{3.11}$$

By instituting the Green's function into Eq. (3.7), the retarded correlation function would be calculated. When there is no spin-orbit coupling, the normal Green's function is simplified to

$$G_N(\boldsymbol{k}, i\omega_l) = -\frac{1}{i\omega_l - \xi_{\boldsymbol{k}}/\hbar}\sigma_0. \tag{3.12}$$

Then the spin susceptibility is calculated as

$$Q_{ij}(\boldsymbol{q}, i\omega_n) = 2\delta_{ij}\left(\frac{g\mu_B}{2}\right)^2 \frac{k_B T}{\hbar}\sum_{\omega_l}\int \frac{d\boldsymbol{k}}{(2\pi)^d}\frac{1}{i\omega_l - \xi_{\boldsymbol{k}_-}/\hbar}\frac{1}{i(\omega_l + \omega_n) - \xi_{\boldsymbol{k}_+}/\hbar} \tag{3.13}$$

$$\chi_N = \lim_{i\omega_n \to 0}\lim_{\boldsymbol{q}\to 0}\chi_{\mu\nu}(\boldsymbol{q}, i\omega_n) = \left(\frac{g\mu_B}{2}\right)^2 N_0\ 2\delta_{\mu\nu}, \tag{3.14}$$

where N_0 is the density of states at the Fermi level. The summation of Matsubara frequency is carried out by using

$$T\sum_{\omega_n}\frac{1}{i\omega_n - a} = n_F(a) - \frac{1}{2}. \tag{3.15}$$

where n_F is the Fermi–Dirac probability distribution function. The spin susceptibility is independent of the temperature, which is called the Pauli paramagnetism and is a characteristic feature of normal metals.

3.2.2 Spin-singlet state

The spin susceptibility depends on temperature in the superconducting phase below T_c. For an even-parity spin-singlet superconductor, the pair potential is given by

$$H_\Delta(\boldsymbol{k}) = d_{0,\boldsymbol{k}} i\sigma_2, \tag{3.16}$$

with $d_{0,-\boldsymbol{k}} = d_{0,\boldsymbol{k}}$. Then the normal Green's function is calculated as

$$G(\boldsymbol{k}, i\omega_n) = \frac{1}{h_0^2 - h_1^2|\boldsymbol{L}_{\boldsymbol{k}}|^2}\left(h_0\sigma_0 + h_1\boldsymbol{L}_{\boldsymbol{k}}\cdot\boldsymbol{\sigma}\right), \tag{3.17}$$

$$h_0 = (i\omega_n - \xi_k) - \frac{d_{0,\boldsymbol{k}}^2}{(i\omega_n + \xi_k)^2 - |\boldsymbol{L}_{\boldsymbol{k}}|^2}(i\omega_n + \xi_k), \tag{3.18}$$

$$h_1 = 1 - \frac{d_{0,\boldsymbol{k}}^2}{(i\omega_n + \xi_k)^2 - |\boldsymbol{L}_{\boldsymbol{k}}|^2}. \tag{3.19}$$

The anomalous Green's function is

$$F(\boldsymbol{k}, i\omega_n) = -\frac{d_{0,\boldsymbol{k}}}{f_0^2 - f_1^2|\boldsymbol{L}_{\boldsymbol{k}}|^2}\left(f_0\sigma_0 + f_1\boldsymbol{L}_{\boldsymbol{k}}\cdot\boldsymbol{\sigma}\right)i\sigma_2, \tag{3.20}$$

$$f_0 = \omega_n^2 + \xi_k^2 + |\boldsymbol{L}_{\boldsymbol{k}}|^2 + d_{0,\boldsymbol{k}}^2, \tag{3.21}$$

$$f_1 = -2\xi_k. \tag{3.22}$$

From the Eqs. (3.7) and (3.8), the spin susceptibility is calculated to

$$\chi_{ii} = -\left(\frac{g\mu_B}{2}\right)^2 \frac{k_B T}{\hbar^2} \sum_{\omega_l} \int \frac{d\boldsymbol{k}}{(2\pi)^3} \times \left[\left(\frac{1}{h_0^2 - h_1^2|\boldsymbol{L}_{\boldsymbol{k}}|^2}\right)^2 2\left(h_0^2 + 2h_1^2 L_{\boldsymbol{k},i}^2 - h_1^2|\boldsymbol{L}_{\boldsymbol{k}}|^2\right) + \left(\frac{d_{0,\boldsymbol{k}}}{f_0^2 - f_1^2|\boldsymbol{L}_{\boldsymbol{k}}|^2}\right)^2 2\left(f_0^2 + 2f_1^2 L_{\boldsymbol{k},i}^2 - f_1^2|\boldsymbol{L}_{\boldsymbol{k}}|^2\right)\right] \tag{3.23}$$

for $i = j$, and

$$\chi_{i\neq j} = -\left(\frac{g\mu_B}{2}\right)^2 \frac{k_B T}{\hbar^2} \sum_{\omega_l} \int \frac{d\boldsymbol{k}}{(2\pi)^3} \times \left[\left(\frac{1}{h_0^2 - h_1^2|\boldsymbol{L}_{\boldsymbol{k}}|^2}\right)^2 4h_1^2 L_{\boldsymbol{k},i} L_{\boldsymbol{k},j} + \left(\frac{d_{0,\boldsymbol{k}}}{f_0^2 - f_1^2|\boldsymbol{L}_{\boldsymbol{k}}|^2}\right)^2 4f_1^2 L_{\boldsymbol{k},i} L_{\boldsymbol{k},j}\right] \tag{3.24}$$

for $i \neq j$.

When there is no spin-orbit coupling and the pair potential is s-wave symmetric *i.e.*, $d_{0,\boldsymbol{k}} = \Delta$, the Green's functions become

$$G(\boldsymbol{k}, i\omega_n) = -\frac{i\omega_n + \xi_{\boldsymbol{k}}/\hbar}{\omega_n^2 + (\xi_{\boldsymbol{k}}/\hbar)^2 + (|\Delta|/\hbar)^2}\,\sigma_0 = -\mathcal{G}(\boldsymbol{k}, i\omega_n)\sigma_0, \tag{3.25}$$

$$F(\boldsymbol{k}, i\omega_n) = -\frac{\Delta/\hbar}{\omega_n^2 + (\xi_{\boldsymbol{k}}/\hbar)^2 + (|\Delta|/\hbar)^2} i\sigma_2 = -\mathcal{F}(\boldsymbol{k}, i\omega_n)i\sigma_2 \tag{3.26}$$

and the spin-susceptibility is calculated to be isotropic,

$$\chi_S = \lim_{i\omega_n\to 0}\lim_{\boldsymbol{q}\to 0} \chi_{ij}(\boldsymbol{q}, i\omega_n) = \chi_N \int d\xi \left(-\frac{\partial n(E)}{\partial E}\right). \tag{3.27}$$

And there is no off-diagonal susceptibility. Eq. (3.27) is rewritten as

$$\chi_S = \chi_N \frac{\frac{\beta}{\Delta}\partial_\beta \Delta}{1 + \frac{\beta}{\Delta}\partial_\beta \Delta}, \tag{3.28}$$

where $\beta = 1/(k_B T)$. This representation is called Yoshida's function which shows the temperature-dependence in spin susceptibility of $S = 1/2$ spin-singlet superconductors. The spin susceptibility becomes small when the temperature is lower than the critical temperature because a spin-singlet Cooper pair has no spin $S = 0$ (Fig. 3.1). At $T = 0$, all electrons near the Fermi level form Cooper pairs so that the spin susceptibility becomes zero, *i.e.*, $\chi_S = 0$.

On the other hand, in the presence of SOC, there can exist finite off-diagonal susceptibility as shown in Eq. (3.24). However, when we assume a simple $\boldsymbol{\lambda}$ with only one factor, such as $\boldsymbol{\lambda} = (0, 0, \lambda)$ which corresponds to the loss of a mirror plane ($z \to -z$)[49], the off-diagonal susceptibility is calculated to zero. For the same $\boldsymbol{\lambda}$, the spin susceptibility shows anisotropic behavior, $\chi_{xx} = \chi_{yy} \neq \chi_{zz}$. In Ref. [48], Frigeri *et al* showed that the spin susceptibility rises with the strength of SOC and $\chi_{xx(yy)} = \chi_{zz}/2$ at the zero temperature.

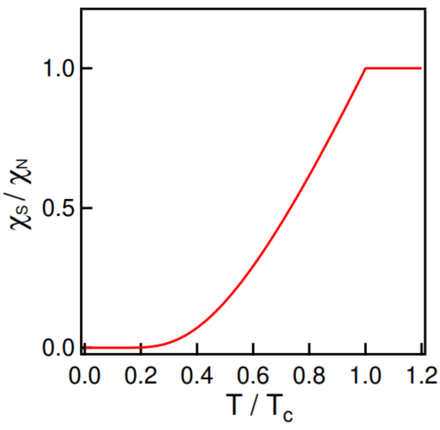

Figure 3.1: Spin susceptibility of a spin-singlet superconductor.

3.2.3 Spin-triplet state

When it comes to a spin-triplet superconductor, a Cooper pair has spin degrees of freedom represented by a $\boldsymbol{d}$-vector in spin space of three dimensions. The pair potential is given by

$$H_\Delta(\boldsymbol{k}) = (\boldsymbol{d}_{\boldsymbol{k}} \cdot \boldsymbol{\sigma})i\sigma_2 \tag{3.29}$$

where $\boldsymbol{d}_{-\boldsymbol{k}} = -\boldsymbol{d}_{\boldsymbol{k}}$. For simplicity, we assume $\boldsymbol{d}_{\boldsymbol{k}} \parallel \boldsymbol{\lambda}_{\boldsymbol{k}}$, which is supposed for $\langle|\boldsymbol{L}_{\boldsymbol{k}}|\rangle_{\boldsymbol{k}} > k_B T_c$.[49] Then the normal Green's function is calculated as

$$G(\boldsymbol{k}, i\omega_n) = \frac{1}{h_{0,t}^2 - |\boldsymbol{h}|^2}\left(h_{0,t}\sigma_0 + \boldsymbol{h}\cdot\boldsymbol{\sigma}\right), \tag{3.30}$$

$$h_{0,t} = (i\omega_n - \xi_k) - \frac{|\boldsymbol{d}_{\boldsymbol{k}}|^2}{(i\omega_n + \xi_k)^2 - |\boldsymbol{L}_{\boldsymbol{k}}|^2}(i\omega_n + \xi_k), \tag{3.31}$$

$$\boldsymbol{h} = \left(1 - \frac{|\boldsymbol{d}_{\boldsymbol{k}}|^2}{(i\omega_n + \xi_k)^2 - |\boldsymbol{L}_{\boldsymbol{k}}|^2}\right)\boldsymbol{L}_{\boldsymbol{k}}. \tag{3.32}$$

The anomalous Green's function is calculated as

$$F(\boldsymbol{k}, i\omega_n) = -\frac{|\boldsymbol{d}_{\boldsymbol{k}}|^2}{f_{0,t}^2 - |\boldsymbol{f}|^2}(f_{0,t}\sigma_0 + \boldsymbol{f}\cdot\boldsymbol{\sigma})i\sigma_2, \tag{3.33}$$

$$f_{0,t} = 2\xi_k(\boldsymbol{d}_{\boldsymbol{k}} \cdot \boldsymbol{L}_{\boldsymbol{k}}), \tag{3.34}$$

$$\boldsymbol{f} = -(\omega_n^2 + \xi_k^2 + |\boldsymbol{L}_{\boldsymbol{k}}|^2 + |\boldsymbol{d}_{\boldsymbol{k}}|^2)\boldsymbol{d}_{\boldsymbol{k}}. \tag{3.35}$$

From the Eqs. (3.7) and (3.8), the spin susceptibility is calculated to

$$\chi_{ii} = -\left(\frac{g\mu_B}{2}\right)^2 \frac{k_B T}{\hbar^2}\sum_{\omega_l}\int\frac{d\boldsymbol{k}}{(2\pi)^3} \times \left[\left(\frac{1}{h_0^2 - |\boldsymbol{h}|^2}\right)^2 2\left(h_0^2 + 2h_i^2 - |\boldsymbol{h}|^2\right) + \left(\frac{|\boldsymbol{d}|^2}{f_{0,t}^2 - |\boldsymbol{f}|^2}\right)^2 2\left(f_{0,t}^2 + 2f_i^2 - |\boldsymbol{f}|^2\right)\right] \tag{3.36}$$

for $i = j$, and

$$\chi_{i\neq j} = -\left(\frac{g\mu_B}{2}\right)^2 \frac{k_B T}{\hbar^2} \sum_{\omega_l} \int \frac{d\boldsymbol{k}}{(2\pi)^3} \left[\left(\frac{1}{h_0^2 - |\boldsymbol{h}|^2}\right)^2 4h_i h_j + \left(\frac{|\boldsymbol{d}|^2}{f_{0,t}^2 - |\boldsymbol{f}|^2}\right)^2 4f_i f_j\right] \tag{3.37}$$

for $i \neq j$.

When there is no SOC and the pair potential is given by

$$\boldsymbol{d}_{\boldsymbol{k}} = \Delta(\boldsymbol{k})\hat{\boldsymbol{d}}, \quad \Delta(\boldsymbol{k}) = -\Delta(-\boldsymbol{k}), \quad |\hat{\boldsymbol{d}}| = 1, \tag{3.38}$$

the Green's function is simplified to

$$G(\boldsymbol{k}, i\omega_n) = -\mathcal{G}(\boldsymbol{k}, i\omega_n)\sigma_0 \tag{3.39}$$

$$F(\boldsymbol{k}, i\omega_n) = -\mathcal{F}(\boldsymbol{k}, i\omega_n)(\hat{\boldsymbol{d}} \cdot \boldsymbol{\sigma})i\sigma_2. \tag{3.40}$$

In this case, the spin susceptibility of a spin-triplet superconductor is summarized to

$$\chi_{\boldsymbol{H}\parallel\boldsymbol{d}}(0,0) = \chi_N \int d\xi \left(-\frac{\partial n(E)}{\partial E}\right) \tag{3.41}$$

$$\chi_{\boldsymbol{H}\perp\boldsymbol{d}}(0,0) = \chi_N \int d\xi \left[\frac{\xi^2}{E^3}\left(-\frac{\partial n(E)}{\partial E}\right) - \frac{\Delta^2}{2E^3}\left(1 - 2n(E)\right)\right] = \chi_N, \tag{3.42}$$

corresponding to the relative direction between the external field $\boldsymbol{H}$ and $\boldsymbol{d}$-vector. We plot the results as a function of a temperature in Fig. 3.2. When the magnetic field is parallel to the $\boldsymbol{d}$-vector, the spin susceptibility is represented by the Yoshida's function. When the magnetic field is perpendicular to the $\boldsymbol{d}$-vector, the spin susceptibility is independent of temperatures. The spin degrees of freedom of a spin-triplet Cooper pair derives the anisotropic magnetic response.

Similarly to the spin-singlet state, when we consider simple $\boldsymbol{\lambda}$ such as $\boldsymbol{\lambda} = (0, 0, \lambda)$, the off-diagonal susceptibility is calculated to zero. In Ref. [48], Frigeri *et al* showed that the spin susceptibilities of spin-singlet and triplet superconductor becomes similar with large SOC strength. Both superconductors show weaker anisotropic behaviors than that of a spin-triplet superconductor with no SOC.

3.3 Magnetic Susceptibility in $J = 3/2$ Superconductor

For a description of $J = 3/2$ superconductors, we have applied the pseudospin representation by the combination of spin and orbital angular momentum. This brings us the general effective Hamiltonian, but also prevent us from the investigation of spin susceptibility. Here, we newly define the magnetic moment of a $J = 3/2$ superconductor in the pseudospin representation,

$$\boldsymbol{m}(\boldsymbol{r}) = \frac{\mu_B}{2} \sum_{\alpha,\beta,\lambda} \psi^\dagger_{\lambda,\alpha}(\boldsymbol{r})(g_1 \boldsymbol{J}_{\alpha,\beta} + g_2 \bar{\boldsymbol{J}}_{\alpha,\beta})\psi_{\lambda,\beta}(\boldsymbol{r}),$$

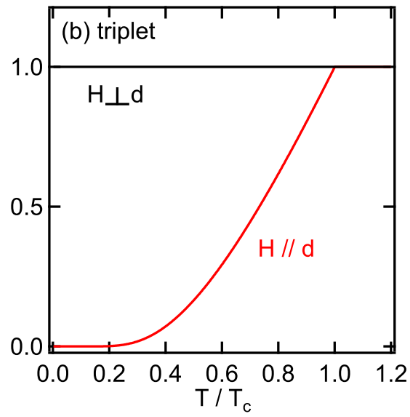

Figure 3.2: Spin susceptibility of a spin-triplet superconductor. The red(black) line refers to the spin susceptibility when the magnetic field is parallel(perpendicular) to the $\boldsymbol{d}$-vector.

with $\bar{J}_\alpha = J_\alpha^3$, from the general Hamiltonian in Eq. (2.8). The parameter g_1 and g_2 depend on materials. Through similar derivation in the previous section for $S = 1/2$ superconductors, the magnetic susceptibility is calculated as

$$\chi_{ij}(\boldsymbol{q}, i\omega_n) = -\left(\frac{\mu_B}{2}\right)^2 \frac{k_B T}{\hbar^2} \sum_{\omega_l} \int \frac{d\boldsymbol{k}}{(2\pi)^d} \\ \times \mathrm{Tr}\ \Big[G(\boldsymbol{k}_-, i\omega_l)\left(g_1 J^i + g_2 \bar{J}^i\right) G(\boldsymbol{k}_+, i\omega_l + i\omega_n)\left(g_1 J^j + g_2 \bar{J}^j\right) \\ + \underset{\sim}{F}(\boldsymbol{k}_-, i\omega_l)\left(g_1 J^i + g_2 \bar{J}^i\right) F(\boldsymbol{k}_+, i\omega_l + i\omega_n)\left(g_1 J^j + g_2 \bar{J}^j\right)^T\Big]. \qquad (3.43)$$

We notice that the definition of magnetic susceptibility includes the effects of orbital susceptibility. We calculate the magnetic susceptibility of an even-parity $J = 3/2$ pseudospin-singlet and -quintet superconductor. By comparing the results with that of a $S = 1/2$ superconductor, we study the magnetic response of a material described by the pseudospin representation.

3.3.1 Normal state

For simplicity, we assume internally isotropic normal Hamiltonian, $H_N = \xi_{\boldsymbol{k}} I_0$ with unit matrix I_0 in pseudospin space, in this chapter. Then the Green's function in the normal state is

$$G_N(\boldsymbol{k}, i\omega_l) = -\frac{1}{i\omega_l - \xi_{\boldsymbol{k}}/\hbar}\gamma^0, \quad F_N(\boldsymbol{k}, i\omega_l) = 0. \qquad (3.44)$$

By substituting the Green's function into Eq. (3.43), the magnetic susceptibility is calculated as

$$\chi_N = N_0 \left(\frac{\mu_B}{2}\right)^2 K^N_{ij}$$
$$K^N_{ij} = \mathrm{Tr}\ \left[\left(g_1 J^i + g_2 \bar{J}^i\right)\left(g_1 J^j + g_2 \bar{J}^j\right)\right] = \left(5g_1^2 + \frac{41}{2} g_1 g_2 + \frac{365}{16} g_2^2\right)\delta_{ij}. \tag{3.45}$$

The susceptibility is independent of the temperature and shows the feature of Pauli paramagnetism, even the specific value is different from that of a $S = 1/2$ superconductor. In this section, we use the same index χ_N to refer to the magnetic susceptibility in the normal state.

3.3.2 Pseudospin-singlet state

The pair potential of a pseudospin-singlet superconductor is given by

$$H_\Delta(\boldsymbol{k}) = \Delta(\boldsymbol{k}) U_T, \quad \Delta(\boldsymbol{k}) = \Delta(-\boldsymbol{k}). \tag{3.46}$$

Then the Green's functions are calculated as

$$G(\boldsymbol{k}, i\omega_n) = -\mathcal{G}(\boldsymbol{k}, i\omega_n)\gamma^0 \tag{3.47}$$
$$F(\boldsymbol{k}, i\omega_n) = -\mathcal{F}(\boldsymbol{k}, i\omega_n) U_T, \tag{3.48}$$

described by the same coefficients in Eq. (3.26), despite of the different pseudospin space. Therefore, Yoshida's function is satisfied also in a $J = 3/2$ pseudospin-singlet superconductor,

$$\chi_S = \chi_N \frac{\frac{\beta}{\Delta}\partial_\beta \Delta}{1 + \frac{\beta}{\Delta}\partial_\beta \Delta}. \tag{3.49}$$

The results are reasonable because a pseudospin-singlet Cooper pair has no spin and does not contribute to the magnetic susceptibility.

3.3.3 Pseudospin-quintet state

The pair potential for a pseudospin quintet state is given by

$$H_\Delta(\boldsymbol{k}) = \Delta(\boldsymbol{k})(\boldsymbol{\eta}\cdot\boldsymbol{\gamma}) U_T, \quad \Delta(\boldsymbol{k}) = \Delta(-\boldsymbol{k}). \tag{3.50}$$

The Green's function is calculated as

$$G(\boldsymbol{k}, i\omega_n) = -\mathcal{G}(\boldsymbol{k}, i\omega_n)\gamma^0, \tag{3.51}$$
$$F(\boldsymbol{k}, i\omega_n) = -\mathcal{F}(\boldsymbol{k}, i\omega_n)(\boldsymbol{\eta}\cdot\boldsymbol{\gamma}) U_T, \tag{3.52}$$
$$\utilde{F}(\boldsymbol{k}, i\omega) = -\mathcal{F}^*(\boldsymbol{k}, i\omega_n) U_T (\boldsymbol{\eta}\cdot\boldsymbol{\gamma}), \tag{3.53}$$

where we have used the relation

$$((\boldsymbol{\eta}\cdot\boldsymbol{\gamma}) U_T)^* = U_T(\boldsymbol{\eta}\cdot\boldsymbol{\gamma}). \tag{3.54}$$

The anomalous Green's function is described by the vector $\boldsymbol{\eta}$ in five-dimensional pseudospin space. By substituting the Green's functions to Eq. (3.43), the susceptibility is calculated as

$$\chi_{\mu\nu}(\boldsymbol{q}, i\omega_n) = -\left(\frac{\mu_B}{2}\right)^2 \frac{k_B T}{\hbar^2} \sum_{\omega_l} \int \frac{d\boldsymbol{k}}{(2\pi)^d} \times \left[\mathcal{G}(\boldsymbol{k}_-, i\omega_l)\mathcal{G}(\boldsymbol{k}_+, i\omega_l + i\omega_n)K^N_{\mu\nu} + \mathcal{F}^*(\boldsymbol{k}_-, i\omega_l)\mathcal{F}(\boldsymbol{k}_+, i\omega_l + i\omega_n)K^A_{\mu\nu}\right], \tag{3.55}$$

where $K^N_{\mu\nu}$ is defined in Eq. (3.45) and

$$K^A_{\mu\nu} = \mathrm{Tr}\left[\left(g_1 J^\mu + g_2 \bar{J}^\mu\right) \boldsymbol{\eta}\cdot\boldsymbol{\gamma} \left(g_1 J^\nu + g_2 \bar{J}^\nu\right) \boldsymbol{\eta}\cdot\boldsymbol{\gamma}\right]. \tag{3.56}$$

We find mainly two features of the magnetic susceptibility in a pseudospin-quintet superconductor. Firstly, we find anisotropy of the magnetic susceptibility, $\chi_{xx} \neq \chi_{yy} \neq \chi_{zz}$, as shown in Fig. 3.3 (a) where we choose the direction of $\boldsymbol{\eta}$ at random. The anisotropy, however, is weaker than that of a $S = 1/2$ spin-triplet superconductor with no SOC in Fig. 3.2. Below T_c, the diagonal term χ_{ii} with $i = x, y, z$ decreases from its value in the normal state but the susceptibility remains finite at $T = 0$. Indeed, it is possible to choose $\boldsymbol{\eta}$ to be symmetric under the cyclic permutation among x, y and z so that the magnetic anisotropy vanishes. In Fig. 3.3 (b), we show the susceptibility for $\boldsymbol{\eta} = (1, 1, 1, 0, 0)$. In this choice of $\boldsymbol{\eta}$ in pseudospin space, there is no particular direction in three dimension and the susceptibility is independent of the direction of a magnetic field. Secondly, the off-diagonal components of the susceptibility are finite in the superconducting state whereas they are zero in the normal state as shown in Fig. 3.3. Thus the off-diagonal magnetic response derived from the anomalous Green's function is a typical property of a pseudospin quintet superconductor.

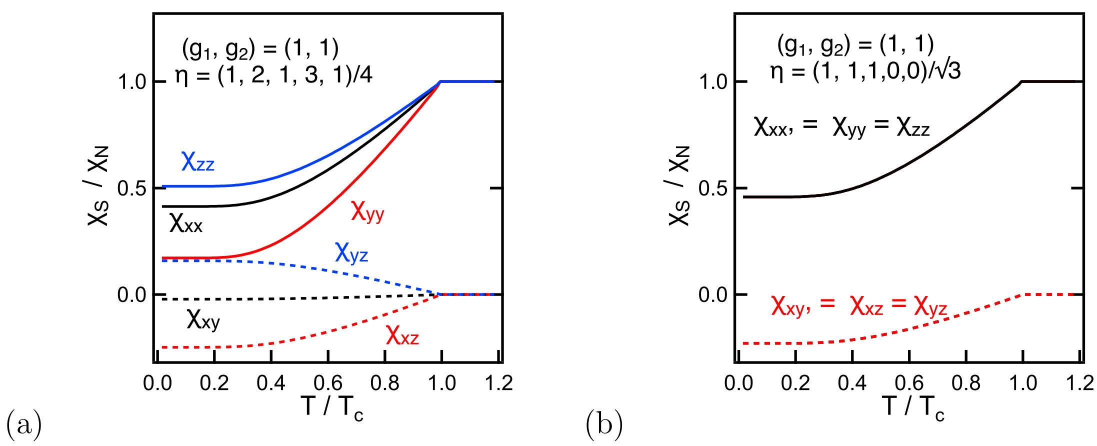

Figure 3.3: Magnetic susceptibility of a pseudospin-quintet superconductor. The material parameters is chosen as $(g_1, g_2) = (1, 1)$. The pair potential is described by 5-dimensional vector, (a) $\boldsymbol{\eta} = (1, 2, 1, 3, 1)/4$ and (b) $\boldsymbol{\eta} = (1, 1, 1, 0, 0)/\sqrt{3}$, respectively. The solid lines refer diagonal elements and the dotted lines refer off-diagonal elements of the tensor χ_{ij}.

The two main features of the magnetic susceptibility originate from the contribution by orbital angular momentum in pseudospin. The high pseudospin results in the anisotropy of magnetic susceptibility, but at the same time, spin-orbit coupling makes it weaker as discussed in Sec. 3.2. The magnetic field $\boldsymbol{H}$ is in three dimension, whereas the $\boldsymbol{\eta}$ is in five dimension. Thus the two vectors are not properly aligned always and this property partially explains the weak anisotropy. The non-trivial value of off-diagonal element is specific result in $J = 3/2$ superconductors. The magnetic moment can be finite in the direction perpendicular to the external magnetic field. Even the off-diagonal term can be finite also for a $S = 1/2$ superconductor with SOC as shown in Eqs. (3.37) and (3.24), it disappears for probable examples.

Finally, we briefly discuss the effects of material parameters (g_1, g_2) on the magnetic susceptibility. We choose $(g_1, g_2) = (1, 0)$ and $(0, 1)$ in Fig. 3.4 (a) and (b), respectively. The parameter choices do not make any qualitative difference in the results. Thus we conclude that the two features discussed above is independent of material parameters.

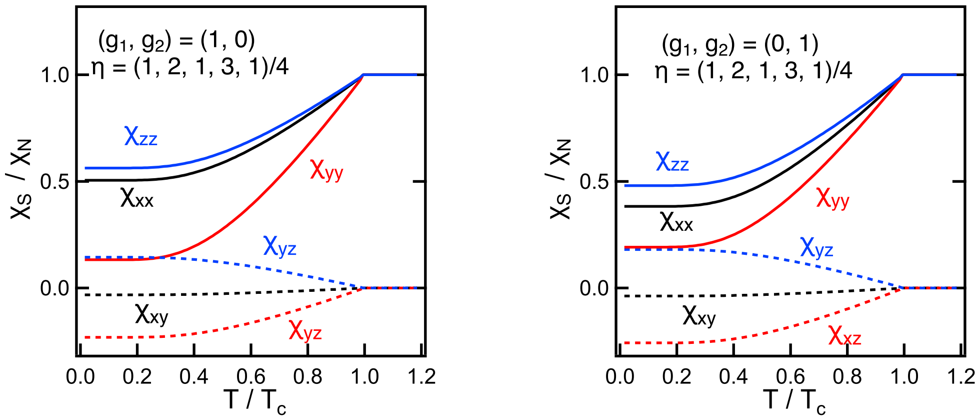

Figure 3.4: Magnetic susceptibility of a pseudospin-quintet superconductor with different choice of the material parameters, (g_1, g_2).

3.4 Summary

We investigated the magnetic susceptibility of $J = 3/2$ superconductors in the pseudospin quintet states. We calculated the magnetic susceptibility within the linear response to an external magnetic field. We found mainly two features in the magnetic susceptibility: the weak anisotropy of the response and the existence of off-diagonal response in three dimensional space of magnetic fields. A Cooper pair at high-angular momentum $J = 2$ is described by a five-dimensional vector $\boldsymbol{\eta}$ in pseudospin space. Namely, the dimension of the space in magnetic field and that in pseudospin do not match to each other. This mismatch is the the origin of the two characteristic feature in the magnetic susceptibility. Thus we also concluded that most of superconductors in pseudospin-quintet state commonly show the two characteristic features.

Chapter 4

Josephson Effect

4.1 Introduction

The Josephson effect is a fundamental property of superconductors through the tunneling of Cooper pairs. We discuss the Josephson effect in a superconductor / insulator / superconductor(SIS) junction consisting of two superconductors.[50] The Josephson current flows from one superconductor to the other via the insulator. The current is dissipationless and originated from the superconducting phase difference of two superconductors.

Just below the superconducting transition temperature T_c, the current-phase $(I - \varphi)$ relationship,

$$I = I_1 \sin\varphi - I_2 \sin 2\varphi, \tag{4.1}$$

is realized in all Josephson junctions consisting of time-reversal symmetry respecting materials. The phase difference is given by $\varphi = \varphi_L - \varphi_R$ for the superconducting phase of the one(the other) superconductor, $\varphi_L(\varphi_R)$, respectively. The Josephson current reflects sensitively the pair potentials in two superconductors. Especially, selection rule, a rule which determines whether the lowest order Josephson current I_1 flows or not, considers the relative symmetry of Cooper pairs in the both sides. The second term I_2, on the other hand, is nonzero for most of the Josephson junctions.

In this chapter, we investigate how the enriched pseudospin-state of a $J = 3/2$ superconductor effects the selection rule on the Josephson current. Therefore, we consider only the lowest order term, $I_1 \sin\varphi$. Before we investigate $J = 3/2$ superconductors, we present the method to calculate the Josephson current and the selection rule for a junction of two $S = 1/2$ superconductors. This gives a fine reference to study the selection rule of two $J = 3/2$ superconductors. Then we will make clear the selection rules among even-parity $J = 3/2$ superconducting states. The effects of a pseudospin-active interface on the selection rule are discussed as well as those of odd-frequency Cooper pairs generated by pseudospin-dependent band structures.

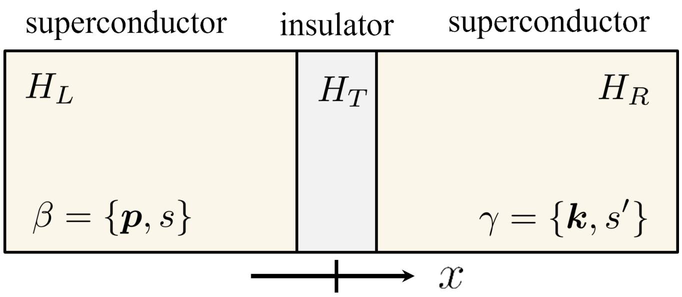

Figure 4.1: The schematic view of a SIS Josephson junction.

4.2 Josephson Current in $S = 1/2$ superconductor

4.2.1 Current formula

We introduce the method to calculate Josephson current in terms of the Green's function. We shows a schematic view of a SIS junction in Fig. 4.1. The interface is located at $x = 0$ and the Josephson current would flows in the x direction. The Hamiltonian of the SIS junction consists of three components,

$$H = H_L + H_R + H_T, \tag{4.2}$$

$$H_T = \sum_{\beta,\gamma} (t_{\gamma\beta} c^\dagger_\gamma c_\beta + t_{\beta\gamma} c^\dagger_\beta c_\gamma), \tag{4.3}$$

where $H_L(H_R)$ is the BdG Hamiltonian of the left(right) superconductor. H_T is a tunneling Hamiltonian which describes the tunneling between two superconductors, where $\beta = \{\boldsymbol{p}, s\}(\gamma = \{\boldsymbol{k}, s'\})$ is a combined index for an electron in the left(right) superconductor. To satisfy the Hermicity of the Hamiltonian, $t^*_{\beta\gamma} = t_{\gamma\beta}$ is required.

The electric Josephson current through the junction is derived by the linear response theory with respect to the tunneling Hamiltonicn, H_T.[51] The result is expressed as

$$I = -2e \, \mathrm{Im} \, T \sum_{\omega_n} \sum_{\boldsymbol{k},\boldsymbol{p}}{}' \mathrm{Tr} \left[t^*_{-\boldsymbol{p},-\boldsymbol{k}} \, \underset{\sim}{F}^R(\boldsymbol{k}, i\omega_n) \, t_{\boldsymbol{k},\boldsymbol{p}} \, F^L(\boldsymbol{p}, i\omega_n) \right], \tag{4.4}$$

where T refers the temperature, Tr means the summation over the pseudospin space, $F^{L(R)}$ is the anomalous Green's function of the left(right) superconductor. $t_{\boldsymbol{k},\boldsymbol{p}}$ is a matrix with the tunnel elements, $\{t_{\boldsymbol{k},\boldsymbol{p}}\}_{s,s'} = t_{\beta\gamma}$. The tunnel event happens between two states on the Fermi surface : one is a state at $k_F \hat{\boldsymbol{p}}$ in the left superconductor and the other is a state at $k_F \hat{\boldsymbol{k}}$ in the right superconductor. The coefficients t_i are real numbers for $i = 0 - 3$. The summation $\sum'_{\boldsymbol{k}}$ is carried out over $\boldsymbol{k}$ for $k_x > 0$. The current formula in Eq. (4.4) is modified under the assumption that the tunnel elements are independent of the wave numbers as

$$t_{\boldsymbol{k},\boldsymbol{p}} = \mathbb{T}_+ \, \delta_{\hat{\boldsymbol{k}},\hat{\boldsymbol{p}}}, \quad \mathbb{T}_\pm = t_0 \pm \sum_{i=1}^{3} t_i \sigma_i, \tag{4.5}$$

where $\delta_{\hat{\boldsymbol{k}},\hat{\boldsymbol{p}}}$ implies the presence of the translation symmetry in the direction parallel to the interface. The element t_0 denotes the tunnel amplitude preserving spin, whereas t_i

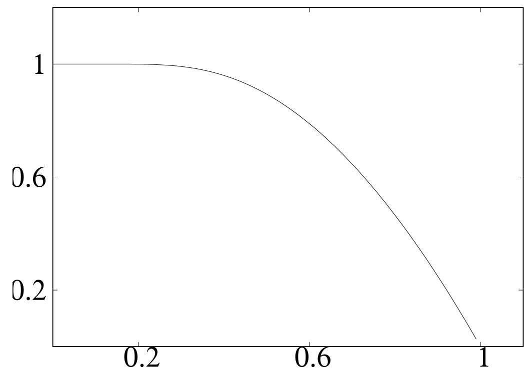

Figure 4.2: The amplitude of the Josephson current between two spin-singlet superconductors plotted over the temperature.

for $i = 1 - 3$ refers to a Zeeman field that couples the angular momentum of an electron. The coefficients t_i for $i = 0 - 3$ are material dependent. The complex conjugation of the hopping element is represented by

$$t^*_{-\boldsymbol{k},-\boldsymbol{p}} = -(i\sigma_2)\mathbb{T}_+ (i\sigma_2)\, \delta_{\hat{\boldsymbol{k}},\hat{\boldsymbol{p}}} = \mathbb{T}_-\, \delta_{\hat{\boldsymbol{k}},\hat{\boldsymbol{p}}}. \tag{4.6}$$

The Josephson current in Eq. (4.4) is transformed to

$$I = 2e\, \mathrm{Im} {\sum_{\boldsymbol{k},\boldsymbol{p}}}' e^{i\varphi}\, T \sum_{\omega_n} \mathrm{Tr}\left[\mathbb{T}'\, \mathbb{F}^R(\boldsymbol{k}, -i\omega_n)\, \mathbb{T}_+\, \mathbb{F}^L(\boldsymbol{p}, i\omega_n)\right] \delta_{\hat{\boldsymbol{k}},\hat{\boldsymbol{p}}}, \tag{4.7}$$

$$\mathbb{T}' = (i\sigma_2)\mathbb{T}_-(i\sigma_2)^{-1} = t_0 + t_1\sigma_1 - t_2\sigma_2 + t_3\sigma_3. \tag{4.8}$$

where $F(\boldsymbol{k}, i\omega_n) = \mathbb{F}(\boldsymbol{k}, i\omega_n)i\sigma_2$. For a while, we consider s-wave superconductors with simple band structure as $H_N(\boldsymbol{k}) = (\varepsilon_0(\boldsymbol{k}) - \mu)I_{2\times 2}$. We also assume that the tunneling Hamiltonian is independent of spin, i.e. $\mathbb{T}_\pm = t_0 I_{2\times 2}$.

4.2.2 Selection rule

We summarize the selection rule of the Josephson current between two $S = 1/2$ superconductors. The results clearly show how the selection rule reflects the relative symmetry of pair potentials in two superconductors. As the most simple case, we assume a Josephson junction between two s-wave spin-singlet superconductors represented by pair potentials which are identical to each other, $H_\Delta^{R(L)} = \Delta i\sigma_2\, e^{i\varphi_{R(L)}}$. Then the Josephson current is calculated from Eq. (4.4),

$$I_{\mathrm{SS}} = \frac{\pi\Delta}{2eR_N} \tanh\left(\frac{\Delta}{2T}\right) \sin\varphi, \tag{4.9}$$

$$R_N^{-1} = 4 \times 2\pi e^2 \left(N_0 t_0\right)^2, \tag{4.10}$$

where R_N is the normal resistance of the junction. The expression of the current is identical to the Ambegaokar-Baratoff's formula (Fig.4.2).[52] Finite Josephson current flows if there exist the difference between two superconducting phases but trivially, does not flow at the temperature higher than the critical temperature.

We also consider a junction between two spin-triplet superconductors. With pair potentials $H_\Delta^{L(R)}(\boldsymbol{k}) = \Delta(\boldsymbol{d}_{\boldsymbol{k}}^{L(R)} \cdot \boldsymbol{\sigma})\, i\sigma_2\, e^{i\varphi_{L(R)}}$, the Josephson current is calculated as

$$I_{\mathrm{TT}} = I_1 \frac{\left\langle \boldsymbol{d}_{\boldsymbol{k}}^L \cdot \boldsymbol{d}_{\boldsymbol{k}}^R \right\rangle_{\hat{\boldsymbol{k}}}}{d_l\, d_r} \sin\varphi, \tag{4.11}$$

$$d_{l(r)} = \sqrt{\left\langle \left\{ \boldsymbol{d}^{L(R)}(\hat{\boldsymbol{k}}) \right\}^2 \right\rangle_{\hat{\boldsymbol{k}}}} \tag{4.12}$$

where $\langle\rangle_{\boldsymbol{k}}$ refers the average over the Fermi surface,

$$\langle X \rangle_{\hat{\boldsymbol{k}}} = \frac{1}{\pi} \int_0^{\pi} d\theta \sin^2\theta \int_{-\pi/2}^{\pi/2} d\phi \cos\phi\, X(\hat{\boldsymbol{k}}), \tag{4.13}$$

where $k_x = k_F \sin\theta\cos\phi > 0$, $k_y = k_F \sin\theta \sin\phi$ and $k_z = k_F\cos\theta$. There are two kinds of selection rule which determine possible Josephson coupling: one is the selection rule for spin and the other is that for orbital. The former is about to the relative symmetry of spin-state. If the spin-states of two superconductors are perpendicular to each other, *i.e.*, $\boldsymbol{d}_{\boldsymbol{k}}^L \perp \boldsymbol{d}_{\boldsymbol{k}}^R$, the Josephson current does not flow. The later is applied to the orbital state. Even though the spin states are not perpendicular, the average in Eq. (4.11), $\langle \boldsymbol{d}_{\boldsymbol{k}}^L \cdot \boldsymbol{d}_{\boldsymbol{k}}^R \rangle_{\hat{\boldsymbol{k}}}$, can be zero due to the orbital degrees of freedom. This selection rule is also applied to a junction of two spin-singlet superconductors, if the pair potential is not isotropic.

The two Josephson junction we discussed consists of two superconductors with pair potentials corresponding to the same angular momentum on both sides, singlet-singlet junction and triplet-triplet junction. A junction between superconductors corresponding to different angular momentum derives interesting results. Basically, with magnetically inactive insulator, no Josephson current flows because the pairing states on both sides are perpendicular each other in the spin-state. However, finite current can flow by adopting a magnetically active insulator for Josephson coupling.[53] Fig. 4.3 refers a junction between superconductors with the pair potentials

$$H_\Delta^L(\boldsymbol{k}) = (\boldsymbol{d}_{\boldsymbol{k}} \cdot \boldsymbol{\sigma})\, i\sigma_2, \tag{4.14}$$

$$H_\Delta^R(\boldsymbol{k}) = \Delta_{s,\boldsymbol{k}}\, i\sigma_2 e^{-i\phi}. \tag{4.15}$$

Using the tunneling perturbation theory, the Josephson current is calculated as

$$I \propto \boldsymbol{d} \cdot \boldsymbol{M} \cos\phi. \tag{4.16}$$

The lowest order term is proportional to $\cos\phi$ because TRS is broken. The magnetization $\boldsymbol{M}$ in the insulator acts to change the spin-state of tunneling Cooper pairs and relaxes the selection rule. However, when the magnetization is perpendicular to $\boldsymbol{d}$-vector, the action does not derive any Josephson coupling between pairing states and Josephson current does not flow. The amplitudes of the magnetization do not affect the selection rule, which only concerns the existence of finite current.

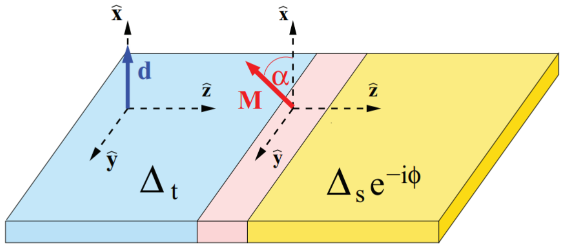

Figure 4.3: A schematic view of a Josephson junction consisting of spin-triplet/singlet superconductors and a magnetically active insulator at $z = 0$.[53] α is the angle between the $\boldsymbol{d}$-vector and the magnetization $\boldsymbol{M}$ in the insulator.

4.3 Josephson Current in $J = 3/2$ Superconductor

In the previous section, we checked that the selection rule deeply related with symmetries of Cooper pairs in the case of $S = 1/2$ superconductors. However, in the case of $J = 3/2$ superconductors, the possibility of pseudospin-quintet and septet pairs makes the relation complex. Even-parity Cooper pair can be in pseudospin-quintet state as well as pseudospin-singlet state so that the effect of the high angular momentum of quintet should be investigated. In this section, we will make clear how the selection rule changes for the Josephson junction between two even-parity $J = 3/2$ superconductors. We also show the effects of a magnetically active junction interface to the selection rule. Finally, we discuss subdominant pairing correlations generated by odd-frequency pairs.

4.3.1 Selection rule

Basically, we can use the current formula derived in the previous section to calculate the lowest order term of Josephson current. We extend the formula to deal with $J = 3/2$ pseudospin space with the assumption

$$t_{\boldsymbol{k},\boldsymbol{p}} = \mathbb{T}_+ \delta_{\hat{\boldsymbol{k}},\hat{\boldsymbol{p}}}, \quad \mathbb{T}_\pm = t_0 \pm \sum_{i=1}^{3} t_i J_i. \tag{4.17}$$

Then the Josephson current in Eq. (4.4) is calculated as

$$I = 2e\,\mathrm{Im}\sum_{\boldsymbol{k},\boldsymbol{p}}{}' e^{i\varphi}\, T \sum_{\omega_n} \mathrm{Tr}\left[\mathbb{T}'\, \mathbb{F}^R(\boldsymbol{k}, -i\omega_n)\, \mathbb{T}_+\, \mathbb{F}^L(\boldsymbol{p}, i\omega_n)\right] \delta_{\hat{\boldsymbol{k}},\hat{\boldsymbol{p}}}, \tag{4.18}$$

$$\mathbb{T}' = U_T \mathbb{T}_- U_T^{-1} = t_0 + t_1 J_1 - t_2 J_2 + t_3 J_3, \tag{4.19}$$

where $F(\boldsymbol{k}, i\omega_n) = \mathbb{F}(\boldsymbol{k}, i\omega_n) U_T$. For a while, we consider s-wave superconductors with simple band structure described by $H_N(\boldsymbol{k}) = (\varepsilon_0(\boldsymbol{k}) - \mu)\gamma^0$ and the tunneling Hamiltonian independent of pseudospin, i.e. $\mathbb{T}_\pm = t_0 \gamma^0$.

Two pseudospin-singlet states

When both superconductors of a Josephson junction are in pseudospin-singlet state, the Josephson current is expected to satisfy the Ambegaokar-Baratoff formula.[52] When both superconductors have s-wave pair potentials,

$$H^L_\Delta(\boldsymbol{p}) = \Delta^L U_T, \quad H^R_\Delta(\boldsymbol{k}) = \Delta^R U_T, \tag{4.20}$$

the Josephson current in Eq. (4.18) is calculated to

$$I_{\rm SS} = 8e\, t_0^2 \sin\varphi\, T \sum_{\omega_n} K(i\omega_n). \tag{4.21}$$

The summation over momentum is carried out as follows,

$$K(i\omega_n) = \sum_{\boldsymbol{p}}{}' \frac{\Delta^L}{(\Delta^L)^2 + \omega_n^2 + \xi_{\boldsymbol{p}}^2} \sum_{\boldsymbol{k}}{}' \frac{\Delta^R}{(\Delta^R)^2 + \omega_n^2 + \xi_{\boldsymbol{k}}^2}\, \delta_{\hat{\boldsymbol{k}},\hat{\boldsymbol{p}}}, \tag{4.22}$$

$$= \left\langle \int \frac{d\xi_k\, N_0}{(\Delta^L)^2 + \omega_n^2 + \xi_k^2} \int \frac{d\xi_k\, N_0}{(\Delta^R)^2 + \omega_n^2 + \xi_k^2} \Delta^L \Delta^R \right\rangle_{\hat{\boldsymbol{k}}}, \tag{4.23}$$

$$= \frac{\pi N_0}{\sqrt{\omega_n^2 + (\Delta^L)^2}} \frac{\pi N_0}{\sqrt{\omega_n^2 + (\Delta^R)^2}} \times \Delta^L \Delta^R. \tag{4.24}$$

The summation over the momentum is decomposed into two parts. One part is the summation over its amplitude $|\boldsymbol{k}|$, which can be replaced by the integration over $\xi_{\boldsymbol{k}}$. The density of states at the Fermi level is denoted by N_0. The details of the integral is summarized in Appendix. C. The other part is summation over the direction of $\boldsymbol{k}$ on the Fermi surface for $k_x > 0$. The Fermi momentum is obtained from $\varepsilon_0(k_F) - \mu = 0$. Finally the Josephson current is calculated as

$$I_{\rm SS} = I_0 \sin\varphi, \tag{4.25}$$

$$I_0 = \frac{\pi}{eR_N} T \sum_{\omega_n} \left(\frac{\Delta^L}{\sqrt{\omega_n^2 + (\Delta^L)^2}} \right) \left(\frac{\Delta^R}{\sqrt{\omega_n^2 + (\Delta^R)^2}} \right), \tag{4.26}$$

$$R_N^{-1} = 4 \times 2\pi e^2 \left(N_0 t_0\right)^2, \tag{4.27}$$

where R_N, the normal resistance of the junction, is modified because of the high degrees of freedom. As the most simple case, we assume that the amplitudes of the two pair potentials are identical to each other, $\Delta^L = \Delta^R = \Delta$. Then the Josephson current results in

$$I_{\rm SS} = \frac{\pi\Delta}{2eR_N} \tanh\left(\frac{\Delta}{2T}\right) \sin\varphi. \tag{4.28}$$

The expression of the current is identical to the Ambegaokar-Baratoff's formula and the same result with the spin-singlet/singlet SIS junction of two $S = 1/2$ superconductors. It is because pseudospin-singlet Cooper pair has spin-zero, just like a spin-singlet pair.

Two pseudospin-quintet states

We discuss the Josephson effect in a junction consisting of two superconductors in pseudospin-quintet states. In contrast to pseudospin-singlet pair, quintet pair has finite angular momentum 2 and its pseudospin-state is described by a five-dimensional vector $\boldsymbol{\eta}$ and the γ

matrices. First, we consider a junction of two s-wave pseudospin-quintet superconductors given by

$$H_\Delta^L(\boldsymbol{p}) = \Delta^L(\boldsymbol{\eta}^L \cdot \boldsymbol{\gamma})U_T, \quad H_\Delta^R(\boldsymbol{k}) = \Delta^R(\boldsymbol{\eta}^R \cdot \boldsymbol{\gamma})U_T. \tag{4.29}$$

By substituting the anomalous Green's function in Eq. (2.29) to Eq. (4.18), the Josephson current is calculated as

$$I_{\mathrm{QQ}} = I_0 \left(\boldsymbol{\eta}^R \cdot \boldsymbol{\eta}^L\right) \sin\varphi. \tag{4.30}$$

The result indicates that the Josephson current is given by the scalar product of two vectors, *i.e.* $I_{\mathrm{QQ}} \propto \boldsymbol{\eta}^L \cdot \boldsymbol{\eta}^R$, which describes the selection rule due to the pseudospin configuration of Cooper pairs. Josephson current cannot flow between two superconductors when two η vectors are perpendicular each other, for example, that of Cooper pairs corresponding to different representations in Table 2.5. The selection rule for quintet states is similar to that in two spin-triplet superconductors of $S = 1/2$ electrons, but the former is severer. This is because two vectors can be orthogonal to each other more easily in higher dimension.

Additionally, we study a case with two $J = 3/2$ superconductors in which pair potentials are anisotropic in the momentum space,

$$H_\Delta^L(\boldsymbol{p}) = (\boldsymbol{\eta}_{\boldsymbol{p}}^L \cdot \boldsymbol{\gamma})U_T, \quad H_\Delta^R(\boldsymbol{k}) = (\boldsymbol{\eta}_{\boldsymbol{k}}^R \cdot \boldsymbol{\gamma})U_T. \tag{4.31}$$

The Josephson current is calculated as

$$I_{\mathrm{QQ}} = I_1 \frac{\left\langle \boldsymbol{\eta}_{\boldsymbol{k}}^R \cdot \boldsymbol{\eta}_{\boldsymbol{k}}^L \right\rangle_{\hat{\boldsymbol{k}}}}{\eta^R \eta^L} \sin\varphi, \tag{4.32}$$

$$I_1 = \frac{\pi}{eR_N} T \sum_{\omega_n} \frac{\eta^R}{\sqrt{\omega_n^2 + (\eta^R)^2}} \frac{\eta^L}{\sqrt{\omega_n^2 + (\eta^L)^2}}, \tag{4.33}$$

$$\eta^{L(R)} = \sqrt{\left\langle \left(\boldsymbol{\eta}_{\boldsymbol{k}}^{L(R)}\right)^2 \right\rangle_{\hat{\boldsymbol{k}}}}. \tag{4.34}$$

The average of $\left\langle \boldsymbol{\eta}_{\boldsymbol{k}}^R \cdot \boldsymbol{\eta}_{\boldsymbol{k}}^L \right\rangle_{\hat{\boldsymbol{k}}}$ on the Fermi surface leads to additional selection rule for the pair potentials depending on orbital. For example in a case of $\boldsymbol{\eta}_{\boldsymbol{k}}^L \propto e_1(\hat{\boldsymbol{k}})$ and $\boldsymbol{\eta}_{\boldsymbol{k}}^R \propto e_2(\hat{\boldsymbol{k}})$, the Josephson current vanishes irrespective of relative pseudospin configurations of Cooper pairs in the two superconductors because of the selection rule in momentum space $\left\langle e_1(\hat{\boldsymbol{k}}) e_2(\hat{\boldsymbol{k}}) \right\rangle_{\hat{\boldsymbol{k}}} = 0$.

Singlet-quintet states

There is a new possibility of $J = 3/2$ superconductors that a Josephson junction consists of two even-parity superconductors with pair potentials of different angular-momenta. The model is given a junction where a pseudospin-singlet s-wave superconductor is on the left and a pseudospin-quintet superconductor is on the right side. The pair potentials are

$$H_\Delta^L(\boldsymbol{p}) = \Delta^L U_T, \quad H_\Delta^R(\boldsymbol{k}) = \Delta^R(\boldsymbol{\eta} \cdot \boldsymbol{\gamma})U_T. \tag{4.35}$$

The vector $\boldsymbol{\eta}$ is normalized vectors in five-dimensional pseudospin space, *i.e.*, $\sum_{\nu=1-5}|\eta_\nu|^2 = 1$. When the tunneling elements are independent of pseudospin $\mathbb{T}_\pm = t_0\gamma^0$, the lowest order of the Josephson current vanishes by the selection rule due to the pseudospin configuration of Cooper pairs. Because pseudospin of a Cooper pair is $J = 0$ in a singlet superconductor, whereas it is $J = 2$ in a quintet superconductor, the pseudospin states are orthogonal to each other.

For finite Josephson current, we switch on a weak Zeeman field to make the interface magnetically active. Then the tunnel elements become pseudospin dependent and can have finite $t_i(\ll t_0)$ for $i = 1-3$ in Eq. (4.5). The Josephson current is calculated as

$$I_{\text{SQ}} = \frac{2\sqrt{3}t_1t_3\eta_3 + \sqrt{3}(t_1^2+t_2^2)\eta_4 - (t_1^2 - t_2^2 - 2t_3^2)\eta_5}{2t_0^2} \times I_0 \sin\varphi. \tag{4.36}$$

Although the lowest order current can have finite value because of the Zeeman field, the contributions of $\nu = 1, 2$ terms vanish. As far as we study, the current-phase relationship is sinusoidal even if a Zeeman field breaks time-reversal symmetry. The results in Eq. (4.36) imply a possibility of π-junction caused by a magnetically active interface. Also, we find the second order terms in the coefficient t_i of the Josephson current as a feature of $J = 3/2$ superconductors. The second order implies that a magnetic field affects a Cooper pair twice during the tunneling. The reason can be explained by considering two facts that the difference in angular momentum of Cooper pairs is $\delta J = 2$ and that J_i matrices in the tunneling Hamiltonian can change the angular momentum only by $\delta J = 1$ for each operation. Therefore, a Zeeman field affects a Cooper pair twice during the tunneling to compensate for the difference in the angular momenta of Cooper pairs. In contrast, the Josephson current between $S = 1/2$ spin-singlet and triplet superconductor is calculated as Eq. (4.16). Thus the current is written in the first order terms in the coefficients of the spin-dependent tunneling Hamiltonian. This implies that a single operation of a Zeeman field can couple the Cooper pairs with the difference of the angular momentum, $\delta S = 1$. This model clearly features the effect of high-angular momentum of a pseudospin-quintet pairs by the resultant severer selection rule.

4.3.2 Josephson Current via Odd-frequency Pair

In this section, we have assumed that electronic structures are independent of pseudospin, i.e., $H_N(\boldsymbol{k}) = (\varepsilon_0(\boldsymbol{k}) - \mu)\gamma^0$. As we showed by the anomalous Green's function in Eq. (2.34), the Hamiltonian depending on the pseudospin generates odd-frequency Cooper pairs. Here, we discuss Josephson current carried by odd-frequency pair. For simplicity, we consider a superconductor which normal Hamiltonian and pair potential have one pseudospin-dependent term respectively and they are described by

$$H_N(\boldsymbol{k}) = \varepsilon_0(\boldsymbol{k}) - \mu + \varepsilon_\lambda(\boldsymbol{k})\,\gamma^\lambda, \quad H_\Delta(\boldsymbol{k}) = \eta_{\boldsymbol{k}}\,\gamma^\nu U_T. \tag{4.37}$$

When $\lambda = \nu$, $H_N(\boldsymbol{k})$ and $H_\Delta(\boldsymbol{k})$ commute to each other. Then no odd-frequency pairing appears in the anomalous Green's function. When we consider a Josephson junction between such two superconductors, the selection rule in Eq. (4.32) remains valid.

In other hand, the selection rule should be modified when $H_N(\boldsymbol{k})$ and $H_\Delta(\boldsymbol{k})$ do not commute in each superconductor, *i.e.* $\lambda \neq \nu$. In this case, the anomalous Green's function is calculated as

$$F_{\nu\lambda}(\boldsymbol{k}, i\omega_n) = F^{(0)}_{\nu}(\boldsymbol{k}, i\omega_n) + \delta F_{\nu\lambda}(\boldsymbol{k}, i\omega_n), \tag{4.38}$$

$$F^{(0)}_{\nu}(\boldsymbol{k}, i\omega_n) = -\frac{1}{\xi^2_{\boldsymbol{k}} + \omega^2_n + \eta^2_{\boldsymbol{k}}}\eta_{\boldsymbol{k}}\gamma^{\nu}U_T, \tag{4.39}$$

$$\delta F_{\nu\lambda}(\boldsymbol{k}, i\omega_n) = -2i\omega_n \frac{\varepsilon_{\lambda}(\boldsymbol{k})}{(\xi^2_{\boldsymbol{k}} + \omega^2_n + \eta^2_{\boldsymbol{k}})^2}\eta_{\boldsymbol{k}}\gamma^{\nu}\gamma^{\lambda}U_T. \tag{4.40}$$

The details of the derivation are shown in Appendix D. Here we assumed $|\varepsilon_{\lambda}| \ll |\varepsilon_0|$ for simplicity. This assumption does not change the symmetry of the correlations. The extra term $\delta F_{\nu\lambda}$ describes an unusual Cooper pairing correlation belonging to odd-frequency symmetry. Since both $\varepsilon_{\lambda}(\boldsymbol{k})$ and $\eta_{\boldsymbol{k}}$ are even-parity functions, $\delta F_{\nu\lambda}(\boldsymbol{k}, i\omega_n)$ is also an even-parity function. The product $\gamma^{\nu}\gamma^{\lambda}U_T$ suggests that $\delta F_{\nu\lambda}$ is symmetric under the permutation of two pseudospins. To meet the requirement of the Fermi-Dirac statistics of electrons, $\delta F_{\nu\lambda}$ must be odd under the permutation of imaginary times as shown in Eq. (4.40). As a result, $\delta F_{\nu\lambda}$ is confined to be an odd function of the Matsubara frequency.[54] We investigate the Josephson current via an odd-frequency pair described by Eq. (4.40) and changes of the selection rule.

Two identical superconductors

We first consider a junction that consists of two identical superconductors described by Eq. (4.37) and a magnetically inactive barrier with tunnel elements $t_{\boldsymbol{k},\boldsymbol{p}} = t_0\gamma^0\delta_{\hat{\boldsymbol{k}},\hat{\boldsymbol{p}}}$. By substituting the Green's function in Eq. (4.38) into Eq. (4.18), the Josephson current is calculated as

$$I = 2e\, t_0^2 \sin\varphi\, T \sum_{\omega_n} \sum_{\boldsymbol{k},\boldsymbol{p}}{}' \mathrm{Tr}\left[\mathbb{F}^{R(0)}_{\nu}(\boldsymbol{k}, -i\omega_n)\, \mathbb{F}^{L(0)}_{\nu}(\boldsymbol{p}, i\omega_n) + \delta\mathbb{F}^{R}_{\nu\lambda}(\boldsymbol{k}, -i\omega_n)\, \delta\mathbb{F}^{L}_{\nu\lambda}(\boldsymbol{p}, i\omega_n)\right], \tag{4.41}$$

$$= I_0 \sin\varphi \left(1 - \frac{\langle\varepsilon_{\lambda}(\boldsymbol{k})\rangle_{\hat{\boldsymbol{k}}}}{8\eta^2}\right). \tag{4.42}$$

The details of the derivation are shown in Appendix D. The Josephson current is dominated by the first term of Eqs. (4.41)-(4.42) carried by an even-frequency pair. An induced odd-frequency pair carries the Josephson current at the second term in Eqs. (4.41)-(4.42). The contribution of an odd-frequency pair is negative, which is derived from the order of pseudospin matrices in the second term as $\mathrm{Tr}[\gamma^{\nu}\,\gamma^{\lambda}\,\gamma^{\nu}\,\gamma^{\lambda}] = -4$. Namely, the coupling between the induced odd-frequency pairing correlations stabilizes the π-state rather than the 0-state because an odd-frequency pair favors phase difference across the junction due to its paramagnetic property.[46] When the amplitude of odd-frequency correlation in Eq. (4.40) exceeds that of even-frequency component in Eq. (4.39), the junction may undergo the transition to the π-state. However, such a superconducting state is impossible because an odd-frequency Cooper pair is thermodynamically unstable.

Two different superconductors

The junction we consider should be always the 0-state because the even-frequency pairing correlations dominate the Josephson current, as shown in Eq. (4.42). However, it also proposes a possibility of a π-junction in the system consisting of time-reversal symmetric components only, if the dominant term could be deleted. In such a context, we construct a junction to delete the dominant term by the severer pseudospin selection rule and simultaneously for subdominant Josephson current to flow. We choose its left superconductor described by Eq. (4.37) and the right superconductor described by

$$H_N(\boldsymbol{k}) = \varepsilon_0 - \mu + \varepsilon_\nu(\boldsymbol{k})\gamma^\nu, \quad H_\Delta(\boldsymbol{k}) = \eta^R_{\boldsymbol{k}}\, \gamma^\lambda U_T. \tag{4.43}$$

The anomalous Green's function of the right superconductor is described by

$$F_{\lambda\nu}(\boldsymbol{k}, i\omega_n) = F^{(0)}_\lambda(\boldsymbol{k}, i\omega_n) + \delta F_{\lambda\nu}(\boldsymbol{k}, i\omega_n). \tag{4.44}$$

The Josephson current in this junction is calculated as

$$I = 2e\, t_0^2 \, \sin\varphi\, T \sum_{\omega_n} {\sum_{\boldsymbol{k},\boldsymbol{p}}}' \mathrm{Tr}\left[\mathbb{F}^{L(0)}_\nu(\boldsymbol{p}, i\omega_n)\, \mathbb{F}^{R(0)}_\lambda(\boldsymbol{k}, -i\omega_n) + \delta\mathbb{F}^L_{\nu\lambda}(\boldsymbol{p}, i\omega_n)\, \delta\mathbb{F}^R_{\lambda\nu}(\boldsymbol{k}, -i\omega_n)\right], \tag{4.45}$$

$$= \frac{\pi}{eR_N} \langle \varepsilon_\lambda(\boldsymbol{k})\, \varepsilon_\nu(\boldsymbol{k}) \eta^R_{\boldsymbol{k}} \eta^L_{\boldsymbol{k}} \rangle_{\hat{\boldsymbol{k}}}\, \sin\varphi \times T \sum_{\omega_n} \frac{\omega_n^2}{\{\omega_n^2 + (\eta^R)^2\}^{3/2} \{\omega_n^2 + (\eta^L)^2\}^{3/2}}. \tag{4.46}$$

The positive sign of the trace is derived from the order of pseudospin matrices as $\mathrm{Tr}[\gamma^\nu\, \gamma^\lambda\, \gamma^\lambda\, \gamma^\nu] = 4$. The first term in Eq. (4.45) vanishes due to the pseudospin selection rule as expected. The second term is carried by induced odd-frequency and its sign is determined by the momentum dependence of the pair potentials. However, it is calculated as positive or zero if the momentum dependence is s-wave or d-wave symmetric. Unfortunately, we cannot draw any physical picture of why an odd-frequency pair stabilizes the 0-state. Even so, the result of the 0-junction is reasonable, because all the parts of the Josephson junction preserve time-reversal symmetry. The superconducting phase should be uniform at the ground state of such a junction.

4.4 Summary

We discussed the Josephson effect of a $J = 3/2$ superconductor preserves time-reversal and inversion symmetries simultaneously. In the presence of inversion symmetry, $J = 0$ pseudospin-singlet and $J = 2$ pseudospin-quintet state are possible. The Josephson current within the tunnel Hamiltonian description is calculated in terms of the anomalous Green's functions on either side of a junction. We found that the Josephson selection rule for quintet states is stricter than that for well-established $S = 1$ spin-triplet states because of the higher angular momentum of Cooper pairs. A magnetically active junction interface relaxes the selection rule and enables the Josephson coupling between a pseudospin-singlet $J = 0$ superconductor and a pseudospin-quintet $J = 2$ superconductor. We also discussed a Josephson current carried by odd-frequency pairing correlations which are generated by the complex commutation relations among pseudospin tensors. We find that the odd-frequency pairing correlation favors the π-state as long as it is a subdominant pairing correlation in a superconductor. The 0-junction stabilized by odd-frequency Cooper pairs is an open question for further researches.

Chapter 5

Bogoliubov Fermi Surface

5.1 Introduction

Although gapped energy spectra of superconductors, quasiparticle states can exist in the subgap energy region, such as a quasiparticle state at nodes of an unconventional superconductor, that at a vortex core[55, 56], and a zero-energy state at a surface of a topologically nontrivial superconductor[57, 58]. A quasiparticle on the Bogoliubov Fermi surface (BFS) is one of the subgap state in a superconductor which breaks time-reversal symmetry spontaneously.[17, 33] In 2017, Agterberg *et al* showed that line or point nodes of even-parity multi-band superconductors with broken TRS inflates to 2-dimensional BFS (Fig. 5.1).[17] The key ingredient is interband pairing, which is expanded to internally anisotropic pairing.[33] Especially, they showed that the existence of BFS is guaranteed topologically if the superconductor preserve charge-conjugation and parity symmetry. The properties of a quasiparticle on BFS have attracted much attention followed by research on time-reversal symmetry breaking superconducting state in a number of unconventional superconductors. At present, however, the physics of a quasiparticle on the BFS has not been explored yet.

Research on the BFS is proposed its existence for a J=3/2 superconductor, because of the high degrees of freedom originated from the spin-orbit coupling. In this chapter, we discuss BFS in a $J = 3/2$ superconductor and the properties of a quasiparticle on it. First, we explain the stability of BFS in an even-parity $J = 3/2$ superconductor. We focus on the relation between a quasiparitlce on BFS and an odd-frequency pair, because several researches have showed the relation between an odd-frequency pair and subgap states. It has been established in a single-band superconductor that a low-energy quasiparticle below the superconducting gap accompanies an odd-frequency Cooper pair.[54, 37, 8] In a two-band/orbital superconductor, the existence of the BFS enhances the subgap spectra in the density of states. Therefore, a quasiparticle on the BFS is considered to generate an odd-frequency Cooper pair. We will show that this reasoning is correct. Finally, we show that the chirality of an odd-frequency pair inherits to a quasiparticle on the Bogoliubov Fermi surface.

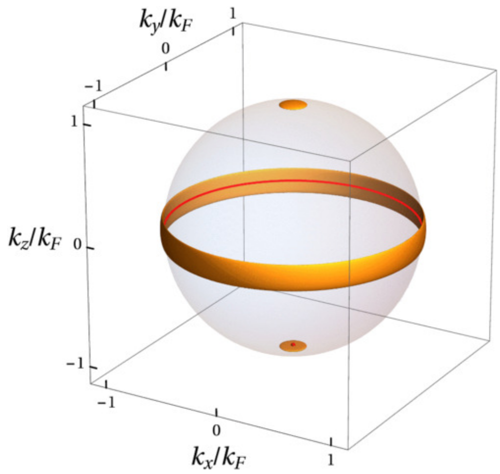

Figure 5.1: Bogoliubov Fermi surfaces (orange) of the superconducting $k_z(k_x + ik_y)$ state.[17] The gray sphere and the red line/dots refer the normal-state Fermi surface and the line/point nodes, respectively. BFS appears as inflated from the nodes.

5.2 Bogoliubov Fermi Surface in $J = 3/2$ superconductors

5.2.1 Stability of BFS

We introduce the method to examine the existence of BFS in an even-parity $J = 3/2$ superconductor, before we investigate a quasiparticle on BFS. We assume the general Hamiltonian in Eq. (2.12) and the even-parity pair potential in Eq. (2.20). Notice that the elements of vector $\boldsymbol{\eta}$ are complex generally, for TRSB pair potential. Also, we adopt the index[33]

$$\begin{aligned} \underline{\varepsilon}_{\boldsymbol{k}} =& (\varepsilon_{\boldsymbol{k},0} - \mu, \boldsymbol{\varepsilon}_{\boldsymbol{k}}), \quad \underline{\eta}_{\boldsymbol{k}} = (\eta_{\boldsymbol{k},0}, \boldsymbol{\eta}_{\boldsymbol{k}}), \\ \langle \underline{a}, \underline{b} \rangle =& a_0 b_0 - \boldsymbol{a} \cdot \boldsymbol{b}. \end{aligned} \tag{5.1}$$

for five-dimensional vector $\boldsymbol{\varepsilon}$ and $\boldsymbol{\eta}$. The most direct method to investigate BFS is to find zero-energy spectrum by the calculation of eigenvalues. However, it is uneasy because of the high-degrees of freedom and the complex factors of TRSB pair potentials.

Therefore, Pfaffian of the BdG Hamiltonian is used instead to examine the existence of BFS. Since zeros of the Pfaffian give the zeros of the excitation spectrum, the sign change of Pfaffian at a certain region in the Brillouin zone indicates the existence of quasiparticle states there. Because Pfaffian is non-negative for the normal state and a continuous function for $\boldsymbol{k}$, we conclude that the existence of negative value refers that of BFS. A general expression of Pfaffian is given in Ref. [33]

$$P(\boldsymbol{k}) = (\langle \underline{\varepsilon}_{\boldsymbol{k}}, \underline{\varepsilon}_{\boldsymbol{k}} \rangle - \langle \underline{\eta}_{\boldsymbol{k}}, \underline{\eta}^*_{\boldsymbol{k}} \rangle)^2 + 4|\langle \underline{\varepsilon}_{\boldsymbol{k}}, \underline{\eta}_{\boldsymbol{k}} \rangle|^2 + \langle \underline{\eta}_{\boldsymbol{k}}, \underline{\eta}_{\boldsymbol{k}} \rangle \langle \underline{\eta}^*_{\boldsymbol{k}}, \underline{\eta}^*_{\boldsymbol{k}} \rangle - \langle \underline{\eta}_{\boldsymbol{k}}, \underline{\eta}^*_{\boldsymbol{k}} \rangle^2. \tag{5.2}$$

Then the topological invariant is defined by

$$(-1)^l = \mathrm{sgn}\, [P(\boldsymbol{k}_-)P(\boldsymbol{k}_+)], \tag{5.3}$$

where $\boldsymbol{k}_-(\boldsymbol{k}_+)$ refers to momenta inside(outside) the Fermi surface, respectively. When the sign of Pfaffian changes across the surface, i.e., $l = 1$, it is a topologically non-trivial BFS.

Unfortunately, it is not easy to obtain the analytical expression for the solutions of $P(\boldsymbol{k}) < 0$. We focus on a promising case of

$$\boldsymbol{\varepsilon}_{\boldsymbol{k}} \cdot \boldsymbol{\eta}_{\boldsymbol{k}} = 0, \tag{5.4}$$

under which the intraband pair potentials have nodes on the Fermi surface [33]. The Pfaffian in such case is represented by,

$$P(\boldsymbol{k}) = \left(\epsilon_{\boldsymbol{k},+}\,\epsilon_{\boldsymbol{k},-} + |\vec{\eta}_{\boldsymbol{k}}|^2\right)^2 - 4 \sum_{n>m>0} |\eta_{\boldsymbol{k},n}|^2\,|\eta_{\boldsymbol{k},m}|^2 \sin^2\left(\phi_{\boldsymbol{k},n} - \phi_{\boldsymbol{k},m}\right), \tag{5.5}$$

$$\epsilon_{\boldsymbol{k},\pm} = \xi_{\boldsymbol{k}} \pm |\boldsymbol{\varepsilon}_{\boldsymbol{k}}|, \quad \eta_{\boldsymbol{k},n} = \eta^{\mathrm{Re}}_{\boldsymbol{k},n} e^{i\phi_{\boldsymbol{k},n}}, \tag{5.6}$$

where $\epsilon_{\boldsymbol{k},\pm} = 0$ characterizes the Fermi surface in the normal state, $\eta^{\mathrm{Re}}_{\boldsymbol{k},n}$ is a real function and $\phi_{\boldsymbol{k},n}$ represents a phase of the n th component. The Pfaffian can be negative when the second term dominates the first one. Although the first term is positive, the components of $\boldsymbol{\varepsilon}_{\boldsymbol{k}}$ can decrease the first term to be smaller than $|\boldsymbol{\eta}_{\boldsymbol{k}}|^2$. The second term remains finite only when the pair potential consists of more than one component and the relative phase of them $\phi_{\boldsymbol{k},n} - \phi_{\boldsymbol{k},m}$ remains finite. It is easy to confirm that such a superconducting state breaks time-reversal symmetry $\mathcal{T}\,\Delta(\boldsymbol{k})\,\mathcal{T}^{-1} \neq \Delta(\boldsymbol{k})$. Therefore, BFS can exist only in the superconducting states with time-reversal symmetry breaking.

5.2.2 BFS and odd-frequency pair

We examined the existence of BFS for even-parity $J = 3/2$ superconductors via the Pfaffian. Then we found that BFS can exist for superconductors of TRSB pair potentials with node and internal degrees of freedom corresponding to pseudospin-dependent normal Hamiltonian and quintet pairing. On the other hand, we know that $[\boldsymbol{\eta}_{\boldsymbol{k}} \cdot \boldsymbol{\gamma}, \boldsymbol{\varepsilon}_{\boldsymbol{k}} \cdot \boldsymbol{\gamma}] \neq 0$ is required for odd-frequency pair to appear from Eq. (2.34). The comparison between two conditions shows that the existence of a quasiparticle on BFS guarantees that of an odd-frequency pair. We can induce that odd-frequency pairing is a broader concept than the formation of BFS.

In the following, we analyze an induced odd-frequency pair in a $J = 3/2$ superconductor with BFS using the correlation function. The correlation function of the induced odd-frequency pair is calculated as below. We assume that the temperature is near the transition temperature T_c so that the relation $|\boldsymbol{\eta}_{\boldsymbol{k}}| \ll T_c$ holds true. Within the first order of $|\boldsymbol{\eta}_{\boldsymbol{k}}|/T_c \ll 1$, the anomalous Green's function in Eq. (2.28) is calculated to be

$$F(\boldsymbol{k}, i\omega_n) = F_{\mathrm{even}}(\boldsymbol{k}, i\omega_n) + F_{\mathrm{odd}}(\boldsymbol{k}, i\omega_n), \tag{5.7}$$

$$F_{\mathrm{even}}(\boldsymbol{k}, i\omega_n) = \frac{-1}{Z_{\mathrm{N}}}\left(\omega_n^2 + \xi_{\boldsymbol{k}}^2 - |\boldsymbol{\varepsilon}_{\boldsymbol{k}}|^2\right) \boldsymbol{\eta}_{\boldsymbol{k}} \cdot \boldsymbol{\gamma}\, U_T, \tag{5.8}$$

$$F_{\mathrm{odd}}(\boldsymbol{k}, i\omega_n) = \frac{-i\omega_n}{Z_{\mathrm{N}}}\left[\boldsymbol{\eta}_{\boldsymbol{k}} \cdot \boldsymbol{\gamma}, \boldsymbol{\varepsilon}_{\boldsymbol{k}} \cdot \boldsymbol{\gamma}\right]_-\, U_T, \tag{5.9}$$

$$Z_{\mathrm{N}} = (\omega_n^2 + \epsilon_{\boldsymbol{k},+}^2)(\omega_n^2 + \epsilon_{\boldsymbol{k},-}^2). \tag{5.10}$$

where we consider a case

$$\boldsymbol{\varepsilon}_{\boldsymbol{k}} \cdot \boldsymbol{\eta}_{\boldsymbol{k}} = 0, \tag{5.11}$$

under which the interband pair potentials have nodes on the Fermi surface. The first term F_{even} belongs to pseudospin-quintet even-parity symmetry class and is linked to the pair potential. The second term F_{odd} belongs to odd-frequency symmetry class and satisfies the relations,

$$F_{\text{odd}}(\boldsymbol{k}, -i\omega_n) = - F_{\text{odd}}(\boldsymbol{k}, i\omega_n), \tag{5.12}$$

$$F_{\text{odd}}(-\boldsymbol{k}, i\omega_n) = F_{\text{odd}}(\boldsymbol{k}, i\omega_n), \tag{5.13}$$

$$F^{\text{T}}_{\text{odd}}(\boldsymbol{k}, i\omega_n) = F_{\text{odd}}(\boldsymbol{k}, i\omega_n). \tag{5.14}$$

Specifically, we analyze three practical cases of superconductors with pair potentials breaking time-reversal symmetry listed in Table. 2.6.[17]

E_g pairing order

We consider the time-reversal symmetry breaking pair potential with $\boldsymbol{h} = (1, i\chi)$ for an E_g symmetry. The pair potential is given by

$$\Delta(\boldsymbol{k}) = \Delta(\Gamma_{3z^2-r^2} + i\chi\Gamma_{x^2-y^2}) = \Delta(\gamma^5 + i\chi\gamma^4)\, U_T, \tag{5.15}$$

where $\chi = \pm 1$ indicates chirality of the pair potential. The corresponding odd-frequency pair is given by substituting Eq. (5.15) to the odd-frequency component in Eq. (5.9),

$$F_{\text{odd}}(\boldsymbol{k}, i\omega_n) = \frac{-i\omega_n \Delta}{Z_{\text{N}}} \left[\gamma^5 + i\chi\gamma^4, \boldsymbol{\varepsilon}_{\boldsymbol{k}} \cdot \boldsymbol{\gamma}\right]_- U_T. \tag{5.16}$$

This equation is decomposed into the irreducible spin matrices in Table 2.5[59]. The details are relegated to Appendix D. The odd-frequency pairing correlation is represented as

$$\begin{aligned} F_{\text{odd}}(\boldsymbol{k}, i\omega_n) = & \frac{-2i\omega_n \Delta}{Z_{\text{N}}} \\ & \times \Bigg\{ \frac{\chi}{\sqrt{5}} \Big[\varepsilon_{\boldsymbol{k},2}\mathcal{J}_1 + \varepsilon_{\boldsymbol{k},3}\mathcal{J}_2 - 2\varepsilon_{\boldsymbol{k},1}\mathcal{J}_3 + i\chi\sqrt{3}(\varepsilon_{\boldsymbol{k},3}\mathcal{J}_2 - \varepsilon_{\boldsymbol{k},2}\mathcal{J}_1)\Big] \\ & \quad - \frac{\chi}{2\sqrt{5}} \Big[\varepsilon_{\boldsymbol{k},2}W_1 + \varepsilon_{\boldsymbol{k},3}W_2 - 2\varepsilon_{\boldsymbol{k},1}W_3 + i\chi\sqrt{3}(\varepsilon_{\boldsymbol{k},3}W_2 - \varepsilon_{\boldsymbol{k},2}W_1)\Big] \\ & \quad + \frac{\chi}{2} \Big[\sqrt{3}(\varepsilon_{\boldsymbol{k},2}W_4 - \varepsilon_{\boldsymbol{k},3}W_5) + i\chi(\varepsilon_{\boldsymbol{k},2}W_4 + \varepsilon_{\boldsymbol{k},3}W_5 - 2\varepsilon_{\boldsymbol{k},1}W_6)\Big] \\ & \quad + \chi(\varepsilon_{\boldsymbol{k},5} + i\chi\varepsilon_{\boldsymbol{k},4})W_7 \Bigg\}. \end{aligned} \tag{5.17}$$

The resulting odd-frequency pairing correlation consists of triplet(J_i terms) and septet(W_i terms) states. An induced odd-frequency pairing correlation inherits the chirality χ of the pair potential. The second line in Eq. (5.17) describes chiral odd-frequency triplet pairs. All the remaining terms describe chiral odd-frequency septet pairs. The emergence of the odd-frequency septet pairs features superconductivity of $j = 3/2$ fermions. It would be worth mentioning that the last term is proportional to an octopolar magnetic order parameter coming from the time-reversal-odd gap product [33]. Therefore, chiral odd-frequency septet pairs are related to a nonunitary pairing state.

T_{2g} pairing order (chiral state)

In the case of T_{2g} symmetry, time-reversal symmetry breaking states are classified into two types: chiral state $\boldsymbol{l} = (1, i\chi, 0)$ $(\chi = \pm 1)$ and cyclic state $\boldsymbol{l} = (1, \omega, \omega^{-1})$ $(\omega = e^{i2\pi/3})$. They are sixfold and eightfold degenerate, respectively.[33] We first examine odd-frequency pairs associated with the chiral state, whose pair potential is given by

$$\Delta(\boldsymbol{k}) = \Delta(\Gamma_{zx} + i\chi\Gamma_{yz}) = \Delta(\gamma^3 + i\chi\gamma^2)\, U_T. \tag{5.18}$$

We find that the resulting odd-frequency pairing correlation in such a chiral superconductor

$$F_{\mathrm{odd}}(\boldsymbol{k}, i\omega_n) = \frac{-i\omega_n\Delta}{Z_{\mathrm{N}}}\left[\gamma^3 + i\chi\gamma^2, \boldsymbol{\varepsilon_k}\cdot\boldsymbol{\gamma}\right]_-\, U_T, \tag{5.19}$$

also inherits the chirality of the pair potential. The odd-frequency pairs can be decomposed into triplet and septet pairing states as

$$\begin{aligned} F_{\mathrm{odd}}(\boldsymbol{k}, i\omega_n) = &\frac{-2i\omega_n\Delta}{Z_{\mathrm{N}}} \\ &\times\Bigg\{\frac{\chi}{\sqrt{5}}\Big[-\varepsilon_{\boldsymbol{k},1}\mathcal{J}_2 - (\varepsilon_{\boldsymbol{k},4} + \sqrt{3}\varepsilon_{\boldsymbol{k},5})\mathcal{J}_1 - i\chi(\varepsilon_{\boldsymbol{k},1}\mathcal{J}_1 - (\varepsilon_{\boldsymbol{k},4} - \sqrt{3}\varepsilon_{\boldsymbol{k},5})\mathcal{J}_2)\Big] \\ &\quad + \frac{\chi}{2\sqrt{5}}\Big[-4\varepsilon_{\boldsymbol{k},1}W_2 + (\varepsilon_{\boldsymbol{k},4} + \sqrt{3}\varepsilon_{\boldsymbol{k},5})W_1 - i\chi(4\varepsilon_{\boldsymbol{k},1}W_1 + (\varepsilon_{\boldsymbol{k},4} - \sqrt{3}\varepsilon_{\boldsymbol{k},5})W_2)\Big] \\ &\quad + \frac{\chi}{2}\Big[(\varepsilon_{\boldsymbol{k},5} - \sqrt{3}\varepsilon_{\boldsymbol{k},4})W_4 - i\chi(\varepsilon_{\boldsymbol{k},5} + \sqrt{3}\varepsilon_{\boldsymbol{k},4})W_5\Big] \\ &\quad + \frac{\chi}{\sqrt{5}}(\varepsilon_{\boldsymbol{k},3} + i\chi\varepsilon_{\boldsymbol{k},2})(\mathcal{J}_3 + 2W_3)\Bigg\}. \end{aligned} \tag{5.20}$$

The last term in Eq. (5.20) is proportion to $4J_z^3 - 7J_z$, which again describes the time-reversal-odd gap product.

T_{2g} pairing order (cyclic state)

Next, we consider the cyclic pair potential $\boldsymbol{l} = (1, \omega, \omega^{-1})$,

$$\begin{aligned} \Delta(\boldsymbol{k}) &= \Delta(\Gamma_{yz} + \omega\Gamma_{zx} + \omega^{-1}\Gamma_{xy}) \\ &= \Delta(\gamma^2 + \omega\gamma^3 + \omega^{-1}\gamma^1)\, U_T, \end{aligned} \tag{5.21}$$

which yields the odd-frequency pairing correlation,

$$F_{\mathrm{odd}}(\boldsymbol{k}, i\omega_n) = \frac{-i\omega_n\Delta}{Z_{\mathrm{N}}}\left[\gamma^2 + \omega\gamma^3 + \omega^{-1}\gamma^1, \boldsymbol{\varepsilon_k}\cdot\boldsymbol{\gamma}\right]_-\, U_T. \tag{5.22}$$

The pairing correlation function involves the phase factors. The results of the decomposition are given by

$$\begin{aligned}
F_{\rm odd}(\boldsymbol{k}, i\omega_n) = &\frac{-2i\omega_n\Delta}{Z_{\rm N}} \\
&\times\Bigg\{ \frac{i}{\sqrt{5}}\Big[(\varepsilon_{\boldsymbol{k},4}+\sqrt{3}\varepsilon_{\boldsymbol{k},5})\mathcal{J}_1+\omega(\varepsilon_{\boldsymbol{k},4}-\sqrt{3}\varepsilon_{\boldsymbol{k},5})\mathcal{J}_2-2\omega^{-1}\varepsilon_{\boldsymbol{k},4}\mathcal{J}_3\Big] \\
&\quad -\frac{i}{2\sqrt{5}}\Big[(\varepsilon_{\boldsymbol{k},4}+\sqrt{3}\varepsilon_{\boldsymbol{k},5})W_1+\omega(\varepsilon_{\boldsymbol{k},4}-\sqrt{3}\varepsilon_{\boldsymbol{k},5})W_2-2\omega^{-1}\varepsilon_{\boldsymbol{k},4}W_3\Big] \\
&\quad -\frac{i}{2}\Big[(\varepsilon_{\boldsymbol{k},5}-\sqrt{3}\varepsilon_{\boldsymbol{k},4})W_4+\omega(\varepsilon_{\boldsymbol{k},5}+\sqrt{3}\varepsilon_{\boldsymbol{k},4})W_5-2\omega^{-1}\varepsilon_{\boldsymbol{k},5}W_6\Big] \\
&\quad +\frac{i}{\sqrt{5}}\Big[\varepsilon_{\boldsymbol{k},1}(\mathcal{J}_2+2W_2)-\varepsilon_{\boldsymbol{k},3}(\mathcal{J}_3+2W_3)+\omega(\varepsilon_{\boldsymbol{k},2}(\mathcal{J}_3+2W_3)-\varepsilon_{\boldsymbol{k},1}(\mathcal{J}_1+2W_1)) \\
&\qquad +\omega^{-1}(\varepsilon_{\boldsymbol{k},3}(\mathcal{J}_1+2W_1)-\varepsilon_{\boldsymbol{k},2}(\mathcal{J}_2+2W_2))\Big]\Bigg\}, \qquad (5.23)
\end{aligned}$$

which consists of both the triplet and septet components.

5.3 Summary

We discussed a quasiparticle on the Bogoliubov Fermi surface (BFS) focusing on the relation with an odd-frequency Cooper pair in a $J = 3/2$ superconductor which breaks time-reversal symmetry. By solving the Gor'kov equation analytically, we showed that a quasiparticle on BFS in a $J = 3/2$ superconducor accompanies an odd-frequency pair characterized by chirality. By comparing the conditions of existence of an odd-frequency pair and the BFS, we found that odd-frequency pairing is a broader concept than the formation of the BFS. Also, the symmetry of odd-frequency Cooper pairs is analyzed in detail by taking realistic pair potentials into account in a cubic superconductor. As a result, we found odd-frequency pairs accompanied by the BFS are pseudospin-triplet and septet pairs characterized by the chirality of the pair potential.

Chapter 6

Conclusion

We theoretically studied the physics of $J = 3/2$ superconductors, where strong spin-orbit interactions make possible a pseudospin $J = 3/2$ electron on the Fermi surface. In the superconducting states in such a material, a Cooper pair consists of two electrons with pseudospin J = 3/2. As a result, the pseudospin of a Cooper pair are classified into a pseudospin $J = 2$ quintet and $J = 3$ septet states, as well as $J = 0$ singlet and $J = 1$ triplet states. The purpose of this thesis is to make clear physics unique to a Cooper pair with such a high angular momentum.

In Ch. 2, we first derive the normal state Hamiltonian for a pseudospin $J = 3/2$ electron which is described by five 4×4 γ-matrices anticommuting one another. In superconducting states, we assume the pair potential belonging to pseudospin-quintet even-parity symmetry class because it is a candidate of the order parameter realized in a half-Heusler semimetal YPtBi. In this thesis, we solve the Gor'kov equation analytically by using the algebra of γ-matrices and obtain both the normal and the anomalous Green's functions. On the basis of the solutions, we discuss the magnetic susceptibility, the Josephson effect, and the relation between a subgap quasiparticle and an odd-frequency Cooper pair.

In Ch. 3, we calculated the magnetic susceptibility of an even-parity $J = 3/2$ superconductor by substituting the obtained Green's function into the linear response formula. The magnetic susceptibility showed weak anisotropy due to the high angular momentum of the pseudospin-quintet state. We also found finite off-diagonal elements in the susceptibility tensor, which is a result of strong spin-orbit couplings. These are considered to be common features to even-parity J = 3/2 superconductors.

In Ch. 4, we discussed the selection rule of a Josephson junction between two $J = 3/2$ superconductors which preserve time-reversal symmetry and inversion symmetry. To calculate the Josephson current, we applied the linear response theory with respect to tunnel Hamiltonian between the two superconductors. As a result, the Josephson current is represented in terms of the anomalous Green's functions on either sides of the Josephson junction. The Josephson selection rule for the quintet states in $J = 3/2$ superconductors states is stricter than that for the spin-triplet states in $S = 1/2$ superconductors. This conclusion is also derived from the high angular momentum of a Cooper pair. We also found that a magnetically active junction interface relaxes the selection rule and an odd-frequency pair can carry a subdominant Josephson current.

In Ch. 5, we showed in an even-parity J = 3/2 superconductor that a quasiparticle on the Bogoliubov Fermi surface accompanies an odd-frequency pair. We conclude that odd-frequency pairing is a broader concept than the formation of the Bogoliubov Fermi surface by comparing the conditions for their appearance. All the Cooper pairing correlations are characterized by the chirality of the pair potential because time-reversal symmetry breaking is a necessary condition for the appearance of a quasiparticle on the Bogoliubov Fermi surface. Our analysis indicated that the induced odd-frequency pairing correlations belong to pseudospin-triplet even-parity and pseudospin-septet even-parity symmetry classes.

Finally, we have discussed physical phenomena unique to a Cooper pair having large angular momentum throughout this thesis. Although there are a number of material parameters in Hamiltonian, our conclusions are insensitive to the parameter choices. Therefore, the characteristic properties discussed in this thesis can be found in most $J = 3/2$ superconductors.

Appendix A

Algebra of $J = 3/2$ Angular Momentum

We list algebra of $J = 3/2$ angular momentum and γ matrices which stem from them. Also, we calculate trace of those matrices for convenience. As the angular momentum matrices, J obey the commutation relations,

$$\begin{aligned} [J_1, J_2] &= iJ_3, \\ [J_2, J_3] &= iJ_1, \\ [J_3, J_1] &= iJ_2. \end{aligned}$$

Traces of multiples of J calculated as

$$\begin{aligned} \mathrm{Tr}\,[J_i] &= 0 \\ \mathrm{Tr}\,[J_iJ_j] &= 5\delta_{ij}, \\ \mathrm{Tr}\,[J_iJ_jJ_k] &= \begin{cases} \frac{5}{2}i & i,j,k = (1,2,3) \\ -\frac{5}{2}i & i,j,k = (1,3,2) \\ 0 & \text{otherwise} \end{cases} . \end{aligned}$$

γ matrices are defined in pseudo-spin space as

$$\gamma^0 = \rho_0\sigma_0$$
$$\gamma^1 = \left(J_xJ_y + J_yJ_x\right)/\sqrt{3} = \begin{pmatrix} 0 & 0 & -i & 0 \\ 0 & 0 & 0 & -i \\ i & 0 & 0 & 0 \\ 0 & i & 0 & 0 \end{pmatrix} = \rho_2\sigma_0$$
$$\gamma^2 = \left(J_yJ_z + J_zJ_y\right)/\sqrt{3} = \begin{pmatrix} 0 & -i & 0 & 0 \\ i & 0 & 0 & 0 \\ 0 & 0 & 0 & i \\ 0 & 0 & -i & 0 \end{pmatrix} = \rho_3\sigma_2$$
$$\gamma^3 = \left(J_xJ_z + J_zJ_x\right)/\sqrt{3} = \begin{pmatrix} 0 & 1 & 0 & 0 \\ 1 & 0 & 0 & 0 \\ 0 & 0 & 0 & -1 \\ 0 & 0 & -1 & 0 \end{pmatrix} = \rho_3\sigma_1$$
$$\gamma^4 = \left(J_x^2 - J_y^2\right)/\sqrt{3} = \begin{pmatrix} 0 & 0 & 1 & 0 \\ 0 & 0 & 0 & 1 \\ 1 & 0 & 0 & 0 \\ 0 & 1 & 0 & 0 \end{pmatrix} = \rho_1\sigma_0$$
$$\gamma^5 = \left(2J_z^2 - J_x^2 - J_y^2\right)/3 = \begin{pmatrix} 1 & 0 & 0 & 0 \\ 0 & -1 & 0 & 0 \\ 0 & 0 & -1 & 0 \\ 0 & 0 & 0 & 1 \end{pmatrix} = \rho_3\sigma_3.$$

The pseudospin matrices can be expressed in terms of γ^j,

$$J_1 = \frac{-i}{2}\left(\sqrt{3}\gamma^2\,\gamma^5 + \gamma^1\,\gamma^3 + \gamma^2\,\gamma^4\right) = \frac{1}{2}(\sqrt{3}\rho_0\sigma_1 + \rho_1\sigma_1 + \rho_2\sigma_2), \tag{A.1}$$
$$J_2 = \frac{i}{2}\left(\sqrt{3}\gamma^3\,\gamma^5 + \gamma^1\,\gamma^2 - \gamma^3\,\gamma^4\right) = \frac{1}{2}(\sqrt{3}\rho_0\sigma_2 - \rho_1\sigma_2 + \rho_2\sigma_1), \tag{A.2}$$
$$J_3 = \frac{i}{2}\left(\gamma^2\,\gamma^3 + 2\,\gamma^1\,\gamma^4\right) = \frac{1}{2}(\rho_0\sigma_3 + 2\rho_3\sigma_0). \tag{A.3}$$

The matrices $\gamma^\nu(\nu = 1-5)$ anti-commute with each other,

$$\gamma^i\gamma^j + \gamma^j\gamma^i = 2\gamma^0\delta_{ij}.$$

Note some relations :

$$\gamma^1\gamma^2\gamma^3\gamma^4\gamma^5 = -1_{4\times4}$$
$$\left(\sum_{\nu=1}^{5}\Delta_\nu\gamma^\nu\right)^2 = \left(\sum_{\nu=1}^{5}\Delta_\nu^2\right)1_{4\times4}.$$

where $1_{4\times4}$ is the identity matrix. Traces of the γ matrices are calculated as

$$\begin{aligned}
\mathrm{Tr}\ \rho_i\sigma_j &= 4\delta_{i0}\delta_{j0}\\
\mathrm{Tr}\ \gamma^i &= 0\\
\mathrm{Tr}\ \gamma^i\gamma^j &= \mathrm{Tr}\left|\begin{array}{c|ccccc}
i\diagdown j & \gamma^1 & \gamma^2 & \gamma^3 & \gamma^4 & \gamma^5\\
\hline
\gamma^1 & \gamma^0 & i\rho_1\sigma_2 & i\rho_1\sigma_1 & -i\rho_3\sigma_0 & i\rho_1\sigma_3\\
\gamma^2 & - & \gamma^0 & -i\rho_0\sigma_3 & i\rho_2\sigma_2 & i\rho_0\sigma_1\\
\gamma^3 & - & - & \gamma^0 & i\rho_2\sigma_1 & -i\rho_0\sigma_2\\
\gamma^4 & - & - & - & \gamma^0 & -i\rho_2\sigma_3\\
\gamma^5 & - & - & - & - & \gamma^0
\end{array}\right| = 4\delta_{ij}\\
\mathrm{Tr}\ \gamma^i\gamma^j\gamma^k &= 0
\end{aligned}$$

For the composition (i, j, k, l) such that $i \le j \le k \le l$,

$$\mathrm{Tr}\ \gamma^i\gamma^j\gamma^k\gamma^l = 4, \qquad \text{for } (i = j = k = l) \text{ or } (i = j < k = l).$$

For the composition (i, j, k, l, m, n) such that $i \le j \le k \le l \le m \le n$,

$$\begin{aligned}
&\mathrm{Tr}\ \gamma^i\gamma^j\gamma^k\gamma^l\gamma^m\gamma^n = 4,\\
&\quad \text{for } (i = j = k = l = m = n) \text{ or } (i = j = k = l < m = n),\ \text{or } (i = j < k = l < m = n).
\end{aligned}$$

Also, we consider the third order factor, $\bar{J}_i = J_i^3$.

$$\begin{aligned}
J_x^3 &= \frac{1}{8}\begin{pmatrix} 0 & 7\sqrt{3} & 0 & 6\\ 7\sqrt{3} & 0 & 20 & 0\\ 0 & 20 & 0 & 7\sqrt{3}\\ 6 & 0 & 7\sqrt{3} & \end{pmatrix}\\
&= \frac{1}{8}(7\sqrt{3}\rho_0\sigma_1 + 13\rho_1\sigma_1 + 7\sigma_2\rho_2) = \frac{-i}{8}(7\sqrt{3}\gamma^2\gamma^5 + 13\gamma^2\gamma^3 + 7\gamma^2\gamma^4)\\
J_y^3 &= -\frac{i}{8}\begin{pmatrix} 0 & 7\sqrt{3} & 0 & -6\\ -7\sqrt{3} & 0 & 20 & 0\\ 0 & -20 & 0 & 7\sqrt{3}\\ 6 & 0 & -7\sqrt{3} & 0 \end{pmatrix}\\
&= \frac{1}{8}(7\sqrt{3}\rho_0\sigma_2 + 7\rho_2\sigma_1 - 13\rho_1\sigma_2) = \frac{i}{8}\left(7\sqrt{3}\gamma^3\gamma^5 - 7\gamma^3\gamma^4 + 13\gamma^1\gamma^2\right), \qquad \text{(A.4)}\\
J_z^3 &= \frac{1}{8}\begin{pmatrix} 27 & 0 & 0 & 0\\ 0 & 1 & 0 & 0\\ 0 & 0 & -1 & 0\\ & 0 & 0 & -27 \end{pmatrix}\\
&= \frac{1}{8}(14\rho_3\sigma_0 + 13\rho_0\sigma_3) = \frac{i}{8}(13\gamma^2\gamma^3 + 14\gamma^1\gamma^2) \qquad \text{(A.5)}
\end{aligned}$$

Appendix B

Linear Response Theory

We summarize the general expression of observable in the presence of time-dependent potential. Consider an expectation value of an observable $\mathcal{O}$ at time t,

$$\begin{aligned}\langle\mathcal{O}\rangle_t &= \langle\psi|U^\dagger\mathcal{O}U|\psi\rangle,\\ U(t) &= e^{-i\mathcal{H}t/\hbar}\end{aligned}$$

In Schrödinger picture, all operators are considered to remain constant, whereas state vectors evolve with time according to

$$\begin{aligned}|\psi(t)\rangle_S &= U(t)|\psi(0)\rangle_S\\ \mathcal{O}_S(t) &= \mathcal{O}_S(0).\end{aligned}$$

Schrödinger equation is

$$i\hbar\frac{\partial|\psi\rangle_S}{\partial t} = \hat{H}|\psi\rangle_S. \tag{B.1}$$

On the other hand, in Heisenberg picture, all state vectors are considered to remain constant at their initial values, whereas operators evolve with time according to

$$\begin{aligned}|\psi(t)\rangle_H &= |\psi(0)\rangle_H\\ \mathcal{O}_H(t) &= U^\dagger(t)\mathcal{O}_H U(t).\end{aligned}$$

The Heisenberg equation of motion is

$$\frac{d\mathcal{O}_H}{dt} = \frac{1}{i\hbar}[\mathcal{O}_H, H] + \frac{\partial\mathcal{O}_H}{\partial t}$$

In interaction picture, state vectors evolve through the Schrödinger picture, but operators evolve through Heisenberg picture. Consider the case where the total Hamiltonian is given by

$$\mathcal{H} = \mathcal{H}_0 + V(t) \tag{B.2}$$

where $\mathcal{H}_0$ is the unperturbed Hamiltonian and $V(t\to-\infty)=0$. The state vectors and the operators are represented as

$$|\psi(t)\rangle_I = e^{iH_0t/\hbar}|\psi(t)\rangle_S. \tag{B.3}$$

The time-dependence of an observable is expressed using the Heisenberg's picture as

$$\mathcal{O}(t) = e^{i\mathcal{H}t/\hbar}\mathcal{O}e^{-i\mathcal{H}t/\hbar}, \tag{B.4}$$

which obeys the Heisenberg's equation of motion,

$$\frac{\partial}{\partial t}\mathcal{O}(t) = \frac{i}{\hbar}[\mathcal{H}, \mathcal{O}(t)]_-. \tag{B.5}$$

The quantum state in the interaction picture obeys

$$i\hbar\frac{\partial}{\partial t}\left\{e^{i\mathcal{H}_0 t/\hbar}|\chi(t)\rangle\right\} = \mathcal{H}\left\{e^{i\mathcal{H}_0 t/\hbar}|\chi(t)\rangle\right\}. \tag{B.6}$$

We find the equation of motion

$$\frac{\partial}{\partial t}|\chi(t)\rangle = -\frac{i}{\hbar}V_I(t)|\chi(t)\rangle, \quad V_I(t) = e^{i\mathcal{H}_0 t/\hbar}Ve^{-i\mathcal{H}_0 t/\hbar}. \tag{B.7}$$

The solution is given by

$$|\chi(t)\rangle = |\chi(t\to-\infty)\rangle - \frac{i}{\hbar}\int_{-\infty}^{t} dt_1 V_I(t_1)|\chi(t_1)\rangle. \tag{B.8}$$

Here we assume that $|\chi_0\rangle = |\chi(t \to -\infty)\rangle$ is the eigenstate of the unperturbed Hamiltonian and that we have known details of $|\chi_0\rangle$. The solution is obtained approximately by

$$|\chi(t)\rangle \sim |\chi_0\rangle - \frac{i}{\hbar}\int_{-\infty}^{t} dt_1 V_I(t_1)|\chi(t_0)\rangle + \left(\frac{i}{\hbar}\right)^2\int_{-\infty}^{t} dt_1 V_I(t_1)\int_{-\infty}^{t_1} dt_2 V_I(t_2)|\chi(t_0)\rangle + \cdots \tag{B.9}$$

The observable at t is then represented by

$$\langle\chi(t)|\mathcal{O}(t)|\chi(t)\rangle \sim \langle\chi_0|\left[1 + \frac{i}{\hbar}\int_{-\infty}^{t} dt_1 V_I(t_1)\right]\mathcal{O}(t)\left[1 - \frac{i}{\hbar}\int_{-\infty}^{t} dt_2 V_I(t_2)\right]|\chi_0\rangle. \tag{B.10}$$

It is calculated by

$$\langle\chi(t)|\mathcal{O}(t)|\chi(t)\rangle \sim \langle\chi_0|\mathcal{O}(0)|\chi_0\rangle - \frac{i}{\hbar}\int_{-\infty}^{t} dt_1 \langle\chi_0|\ [\mathcal{O}(t), V_I(t_1)]\ |\chi_0\rangle \tag{B.11}$$

in the first order of the perturbation. This equation describes the linear response of superconductors to perturbation.

Appendix C

Table for Integrals, Summations and Constants

Here we summarize formulas of integral and summation over the Matsubara frequency, used in this paper.

$$\int_{-\infty}^{\infty} \frac{dx}{x^2+a^2} = \frac{\pi}{a}, \quad \int_{-\infty}^{\infty} \frac{dx}{(x^2+a^2)^2} = \frac{\pi}{2a^3}, \tag{C.1}$$

$$T\sum_{\omega_n} \frac{1}{\omega_n^2+a^2} = \frac{1}{2a}\tanh\left(\frac{a}{2T}\right), \tag{C.2}$$

$$T\sum_{\omega_n} \frac{\omega_n^2}{(\omega_n^2+a^2)^3} = \frac{1}{16a^3}\left[\tanh\left(\frac{a}{2T}\right) - \frac{a}{2T}\cosh^{-2}\left(\frac{a}{2T}\right) + 2\left(\frac{a}{2T}\right)^2 \frac{\tanh\left(\frac{a}{2T}\right)}{\cosh^2\left(\frac{a}{2T}\right)}\right], \tag{C.3}$$

$$\approx \frac{1}{16a^3}\tanh\left(\frac{a}{2T}\right). \tag{C.4}$$

The last equation is approximated in case $T \ll a$. The average of functions in Eq. (2.14) over the Fermi surface give constants,

$$\left\langle e_1^2(\hat{\boldsymbol{k}})\right\rangle_{\hat{\boldsymbol{k}}} = \frac{3}{10}, \quad \left\langle e_2^2(\hat{\boldsymbol{k}})\right\rangle_{\hat{\boldsymbol{k}}} = \frac{1}{8}, \quad \left\langle e_3^2(\hat{\boldsymbol{k}})\right\rangle_{\hat{\boldsymbol{k}}} = \frac{1}{4}, \quad \left\langle e_4^2(\hat{\boldsymbol{k}})\right\rangle_{\hat{\boldsymbol{k}}} = \frac{7}{32}, \quad \left\langle e_5^2(\hat{\boldsymbol{k}})\right\rangle_{\hat{\boldsymbol{k}}} = \frac{5}{32}, \tag{C.5}$$

$$\left\langle e_1(\hat{\boldsymbol{k}})\, e_{\lambda\neq 1}(\hat{\boldsymbol{k}})\right\rangle_{\hat{\boldsymbol{k}}} = \left\langle e_2(\hat{\boldsymbol{k}})\, e_{\lambda\neq 2}(\hat{\boldsymbol{k}})\right\rangle_{\hat{\boldsymbol{k}}} = \left\langle e_3(\hat{\boldsymbol{k}})\, e_{\lambda\neq 3}(\hat{\boldsymbol{k}})\right\rangle_{\hat{\boldsymbol{k}}} = 0, \quad \left\langle e_4(\hat{\boldsymbol{k}})\, e_5(\hat{\boldsymbol{k}})\right\rangle_{\hat{\boldsymbol{k}}} = \frac{\sqrt{3}}{32}. \tag{C.6}$$

Appendix D

Odd-frequency Pairing

Here we first derive the anomalous Green's function in a superconductors in the presence of pseudospin-dependent dispersion. Then we show the derivation of the Josephson current. When a superconductor is described by Eq. (4.37), its anomalous Green's function is calculated as

$$\begin{aligned}\mathbb{F}_{\nu\lambda}(\boldsymbol{k}, i\omega_n) &= \left[-\eta_{\boldsymbol{k}}\gamma^{\nu} + \left(i\omega_n + \xi_{\boldsymbol{k}} + \varepsilon_{\lambda}(\boldsymbol{k})\,\gamma^{\lambda}\right)(\eta_{\boldsymbol{k}}\gamma^{\nu})^{-1}\left(i\omega_n - \xi_{\boldsymbol{k}} - \varepsilon_{\lambda}(\boldsymbol{k})\,\gamma^{\lambda}\right)\right]^{-1}, \\ &= -\left[\left\{\frac{\eta_{\boldsymbol{k}}^2 + \omega_n^2 + \xi_{\boldsymbol{k}}^2 - \varepsilon_{\lambda}^2(\boldsymbol{k})}{\eta_{\boldsymbol{k}}}\gamma^0 - 2i\omega_n\frac{\varepsilon_{\lambda}(\boldsymbol{k})}{\eta_{\boldsymbol{k}}}\gamma^{\lambda}\right\}\gamma^{\nu}\right]^{-1}, \\ &\approx -\frac{\eta_{\boldsymbol{k}}}{\eta_{\boldsymbol{k}}^2 + \omega_n^2 + \xi_{\boldsymbol{k}}^2}\gamma^{\nu} - 2i\omega_n\frac{\varepsilon_{\lambda}(\boldsymbol{k})\eta_{\boldsymbol{k}}}{(\eta_{\boldsymbol{k}}^2 + \omega_n^2 + \xi_{\boldsymbol{k}}^2)^2}\gamma^{\nu}\gamma^{\lambda}. \end{aligned} \tag{D.1}$$

At the last line, we assumed $|\varepsilon_{\lambda}(\boldsymbol{k})| \ll |\varepsilon_0(\boldsymbol{k})|$ for $\lambda = 1 - 5$. The second term refers an odd-frequency pairing.

We construct a Josephson junction with the left superconductor described by Eq. (4.37) and the right superconductor described by

$$\mathbb{E}_{\boldsymbol{k}} = \varepsilon_0(\boldsymbol{k}) + \varepsilon_{\rho}(\boldsymbol{k})\,\gamma^{\rho} - \mu, \quad \mathbb{D}_{\boldsymbol{k}} = \eta_{\boldsymbol{k}}\,\gamma^{\kappa}, \tag{D.2}$$

with $\rho \neq \kappa$. When an insulator is magnetically inactive *i.e.* $\mathbb{T} = t_0\gamma^0$, the Josephson current becomes

$$I = 2e\,t_0^2\,\sin\varphi\,T{\sum_{\boldsymbol{k},\boldsymbol{p}}}' \mathrm{Tr}\left[\mathbb{F}^0_{\nu}(\boldsymbol{k}, -i\omega_n)\,\mathbb{F}^0_{\nu}(\boldsymbol{p}, i\omega_n) + \delta\mathbb{F}_{\nu\lambda}(\boldsymbol{k}, -i\omega_n)\,\delta\mathbb{F}_{\nu\lambda}(\boldsymbol{p}, i\omega_n)\right]\delta_{\hat{\boldsymbol{k}},\hat{\boldsymbol{p}}} \tag{D.3}$$

$$\begin{aligned} =& 8e\,t_0^2\,\sin\varphi\,T\sum_{\omega_n}\left[{\sum_{\boldsymbol{k},\boldsymbol{p}}}'\frac{1}{(\eta^R_{\boldsymbol{k}})^2 + \omega_n^2 + \xi_{\boldsymbol{k}}^2}\frac{1}{(\eta^L_{\boldsymbol{p}})^2 + \omega_n^2 + \xi_{\boldsymbol{p}}^2}\eta^R_{\boldsymbol{k}}\eta^L_{\boldsymbol{p}}\delta_{\nu\kappa}\delta_{\hat{\boldsymbol{k}},\hat{\boldsymbol{p}}}\right. \\ & \left. -4\omega_n^2{\sum_{\boldsymbol{k},\boldsymbol{p}}}'\frac{\varepsilon^R_{\rho}(\boldsymbol{k})}{\{(\eta^R_{\boldsymbol{k}})^2 + \omega_n^2 + \xi_{\boldsymbol{k}}^2\}^2}\frac{\varepsilon^L_{\lambda}(\boldsymbol{p})}{\{(\eta^L_{\boldsymbol{p}})^2 + \omega_n^2 + \xi_{\boldsymbol{p}}^2\}^2}\eta^R_{\boldsymbol{k}}\eta^L_{\boldsymbol{p}}(\delta_{\lambda\rho}\delta_{\nu\kappa} - \delta_{\lambda\kappa}\delta_{\nu\rho})\delta_{\hat{\boldsymbol{k}},\hat{\boldsymbol{p}}}\right] \end{aligned} \tag{D.4}$$

As shown in the equation, there are two cases where finite Josephson current is allowed, $\nu = \kappa$, or $\lambda = \kappa$ and $\nu = \rho$ simultaneously. The condition $\nu = \kappa$ corresponds to the selection rule $I \propto \boldsymbol{q}^L \cdot \boldsymbol{q}^R$.

For the case $\nu = \kappa$, the Josephson current is calculated as

$$I = 8e\, t_0^2 \sin\varphi\, T \sum_{\omega_n} \left[\sum_{\boldsymbol{k},\boldsymbol{p}}{}' \frac{1}{(\eta_{\boldsymbol{k}}^R)^2 + \omega_n^2 + \xi_{\boldsymbol{k}}^2} \frac{1}{(\eta_{\boldsymbol{p}}^L)^2 + \omega_n^2 + \xi_{\boldsymbol{p}}^2} \eta_{\boldsymbol{k}}^R \eta_{\boldsymbol{p}}^L \delta_{\hat{\boldsymbol{k}},\hat{\boldsymbol{p}}} \right.$$
$$\left. -4\omega_n^2 \sum_{\boldsymbol{k},\boldsymbol{p}}{}' \frac{\varepsilon_\rho^R(\boldsymbol{k})}{\{(\eta_{\boldsymbol{k}}^R)^2 + \omega_n^2 + \xi_{\boldsymbol{k}}^2\}^2} \frac{\varepsilon_\lambda^L(\boldsymbol{p})}{\{(\eta_{\boldsymbol{p}}^L)^2 + \omega_n^2 + \xi_{\boldsymbol{p}}^2\}^2} \eta_{\boldsymbol{k}}^R \eta_{\boldsymbol{p}}^L \delta_{\lambda\rho} \delta_{\hat{\boldsymbol{k}},\hat{\boldsymbol{p}}} \right] \tag{D.5}$$

$$= \frac{\pi}{eR_N} \sin\varphi\, T \sum_{\omega_n} \left[\frac{1}{\sqrt{(\eta^R)^2 + \omega_n^2}} \frac{1}{\sqrt{(\eta^L)^2 + \omega_n^2}} \langle \eta_{\boldsymbol{k}}^R \eta_{\boldsymbol{p}}^L \rangle_{\hat{\boldsymbol{k}}} \right.$$
$$\left. -\omega_n^2 \frac{1}{\{(\eta^R)^2 + \omega_n^2\}^{3/2}} \frac{1}{\{(\eta^L)^2 + \omega_n^2\}^{3/2}} \langle \varepsilon_\rho^R(\boldsymbol{k}) \varepsilon_\lambda^L(\boldsymbol{p}) \eta_{\boldsymbol{k}}^R \eta_{\boldsymbol{p}}^L \rangle_{\hat{\boldsymbol{k}}} \delta_{\lambda\rho} \right]. \tag{D.6}$$

If we assume $\eta^R = \eta^L = \Delta$, the Josephson current is simplified as

$$I = \frac{\pi\Delta}{2eR_N} \tanh\left(\frac{\Delta}{2T}\right) \left[\frac{\langle \eta_{\boldsymbol{k}}^R \eta_{\boldsymbol{k}}^L \rangle_{\hat{\boldsymbol{k}}}}{\Delta^2} - \frac{\langle \varepsilon_\rho^R(\boldsymbol{k}) \varepsilon_\lambda^L(\boldsymbol{p}) \eta_{\boldsymbol{k}}^R \eta_{\boldsymbol{p}}^L \rangle_{\hat{\boldsymbol{k}}}}{8\Delta^4} \delta_{\lambda\rho} \right] \sin\varphi. \tag{D.7}$$

The first term is equivalent to the Josephson current without the pseudospin-dependent dispersion, Eq. (4.32). The second term represents the Josephson current carried by induced odd-frequency pairs in the two superconductors. It is finite for $\lambda = \rho$, where symmetries of both superconductors are identical. Its negative sign is derived from $\mathrm{Tr}[\gamma^\nu \gamma^\lambda \gamma^\nu \gamma^\lambda] = -4$.

For $\lambda = \kappa$ and $\nu = \rho$, the Josephson junction consists of two superconductors described by Eq. (4.37) for the left and Eq. (4.43) for the right side. The Josephson current is calculated as

$$I = \frac{\pi}{eR_N} \sin\varphi\, T \sum_{\omega_n} \left[\omega_n^2 \frac{1}{\{(\eta^R)^2 + \omega_n^2\}^{3/2}} \frac{1}{\{(\eta^L)^2 + \omega_n^2\}^{3/2}} \langle \varepsilon_\rho^R(\boldsymbol{k}) \varepsilon_\lambda^L(\boldsymbol{p}) \eta_{\boldsymbol{k}}^R \eta_{\boldsymbol{p}}^L \rangle_{\hat{\boldsymbol{k}}} \right] \tag{D.8}$$

$$= \frac{\pi\Delta}{2eR_N} \tanh\left(\frac{\Delta}{2T}\right) \frac{\langle \varepsilon_\rho^R(\boldsymbol{k}) \varepsilon_\lambda^L(\boldsymbol{p}) \eta_{\boldsymbol{k}}^R \eta_{\boldsymbol{p}}^L \rangle_{\hat{\boldsymbol{k}}}}{8\Delta^4} \sin\varphi. \tag{D.9}$$

For the last line, we assumed $\eta^R = \eta^L = \Delta$. The positive sign is from $\mathrm{Tr}[\gamma^\nu \gamma^\lambda \gamma^\lambda \gamma^\nu] = 4$.

Finaly, we summarize the decomposition of odd-frequency pairing correlation function into triplet and septet components in $j = 3/2$ superconductors with cubic symmetry. We used the following relations

$$
\begin{aligned}
&\gamma^1\gamma^2\, U_T = -\frac{i}{\sqrt{5}}(\mathcal{J}_2 + 2W_2), \quad \gamma^1\gamma^3\, U_T = \frac{i}{\sqrt{5}}(\mathcal{J}_1 + 2W_1),\\
&\gamma^1\gamma^4\, U_T = -\frac{i}{\sqrt{5}}(\mathcal{J}_3 - 2W_3), \quad \gamma^1\gamma^5\, U_T = iW_6,\\
&\gamma^2\gamma^3\, U_T = -\frac{i}{\sqrt{5}}(\mathcal{J}_3 + 2W_3),\\
&\gamma^2\gamma^4\, U_T = \frac{i}{\sqrt{5}}\mathcal{J}_1 - \frac{i}{2\sqrt{5}}W_1 + i\frac{\sqrt{3}}{2}W_4,\\
&\gamma^2\gamma^5\, U_T = i\sqrt{\frac{3}{5}}\mathcal{J}_1 - \frac{i}{2}\sqrt{\frac{3}{5}}W_1 - \frac{i}{2}W_4,\\
&\gamma^3\gamma^4\, U_T = \frac{i}{\sqrt{5}}\mathcal{J}_2 - \frac{i}{2\sqrt{5}}W_2 - i\frac{\sqrt{3}}{2}W_5,\\
&\gamma^3\gamma^5\, U_T = -i\sqrt{\frac{3}{5}}\mathcal{J}_2 + \frac{i}{2}\sqrt{\frac{3}{5}}W_2 - \frac{i}{2}W_5,\\
&\gamma^4\gamma^5\, U_T = -iW_7,
\end{aligned}
\tag{D.10}
$$

in Eqs. (5.17), (5.20), and (5.23).

Bibliography

[1] H Kamerlingh Onnes. Further experiments with liquid helium. c. on the change of electric resistance of pure metals at very low temperatures etc. iv. the resistance of pure mercury at helium temperatures. In *KNAW, Proceedings*, volume 13, pages 1910–1911, 1911.

[2] J. Bardeen, L. N. Cooper, and J. R. Schrieffer. Theory of superconductivity. *Phys. Rev.*, 108:1175–1204, Dec 1957.

[3] H. Tou, Y. Kitaoka, K. Ishida, K. Asayama, N. Kimura, Y. O¯nuki, E. Yamamoto, Y. Haga, and K. Maezawa. Nonunitary spin-triplet superconductivity in upt_3: Evidence from ^{195}pt knight shift study. *Phys. Rev. Lett.*, 80:3129–3132, Apr 1998.

[4] K Ishida, H Mukuda, Y Kitaoka, K Asayama, ZQ Mao, Y Mori, and Y Maeno. Spin-triplet superconductivity in sr 2 ruo 4 identified by 17 o knight shift. *Nature*, 396(6712):658–660, 1998.

[5] Masahiro Manago, Shunsaku Kitagawa, Kenji Ishida, Kazuhiko Deguchi, Noriaki K. Sato, and Tomoo Yamamura. Spin-triplet superconductivity in the paramagnetic ucoge under pressure studied by ^{59}Co nmr. *Phys. Rev. B*, 100:035203, Jul 2019.

[6] M Zahid Hasan and Charles L Kane. Colloquium: topological insulators. *Reviews of modern physics*, 82(4):3045, 2010.

[7] Xiao-Liang Qi and Shou-Cheng Zhang. Topological insulators and superconductors. *Reviews of Modern Physics*, 83(4):1057, 2011.

[8] Yukio Tanaka, Masatoshi Sato, and Naoto Nagaosa. Symmetry and topology in superconductors –odd-frequency pairing and edge states–. *Journal of the Physical Society of Japan*, 81(1):011013, 2012.

[9] Yoichi Ando. Topological insulator materials. *Journal of the Physical Society of Japan*, 82(10):102001, 2013.

[10] Yoichi Ando and Liang Fu. Topological crystalline insulators and topological superconductors: From concepts to materials. *Annu. Rev. Condens. Matter Phys.*, 6(1):361–381, 2015.

[11] Masatoshi Sato and Satoshi Fujimoto. Majorana fermions and topology in superconductors. *Journal of the Physical Society of Japan*, 85(7):072001, 2016.

[12] NP Armitage, EJ Mele, and Ashvin Vishwanath. Weyl and dirac semimetals in three-dimensional solids. *Reviews of Modern Physics*, 90(1):015001, 2018.

[13] PMR Brydon, Limin Wang, M Weinert, and DF Agterberg. Pairing of j= 3/2 fermions in half-heusler superconductors. *Physical review letters*, 116(17):177001, 2016.

[14] Igor Boettcher and Igor F Herbut. Superconducting quantum criticality in three-dimensional luttinger semimetals. *Physical Review B*, 93(20):205138, 2016.

[15] Lucile Savary, Jonathan Ruhman, Jörn WF Venderbos, Liang Fu, and Patrick A Lee. Superconductivity in three-dimensional spin-orbit coupled semimetals. *Physical Review B*, 96(21):214514, 2017.

[16] Igor Boettcher and Igor F. Herbut. Unconventional superconductivity in luttinger semimetals: Theory of complex tensor order and the emergence of the uniaxial nematic state. *Phys. Rev. Lett.*, 120:057002, Feb 2018.

[17] DF Agterberg, PMR Brydon, and C Timm. Bogoliubov fermi surfaces in superconductors with broken time-reversal symmetry. *Physical review letters*, 118(12):127001, 2017.

[18] Jörn WF Venderbos, Lucile Savary, Jonathan Ruhman, Patrick A Lee, and Liang Fu. Pairing states of spin-3 2 fermions: Symmetry-enforced topological gap functions. *Physical Review X*, 8(1):011029, 2018.

[19] Takuto Kawakami, Tetsuya Okamura, Shingo Kobayashi, and Masatoshi Sato. Topological crystalline materials of j= 3/2 electrons: Antiperovskites, dirac points, and high winding topological superconductivity. *Physical Review X*, 8(4):041026, 2018.

[20] Jiabin Yu and Chao-Xing Liu. Singlet-quintet mixing in spin-orbit coupled superconductors with j= 3 2 fermions. *Physical Review B*, 98(10):104514, 2018.

[21] Sayed Ali Akbar Ghorashi, Seth Davis, and Matthew S Foster. Disorder-enhanced topological protection and universal quantum criticality in a spin-3 2 topological superconductor. *Physical Review B*, 95(14):144503, 2017.

[22] Shingo Kobayashi, Ai Yamakage, Yukio Tanaka, and Masatoshi Sato. Majorana multipole response of topological superconductors. *Phys. Rev. Lett.*, 123:097002, Aug 2019.

[23] J. M. Luttinger and W. Kohn. Motion of electrons and holes in perturbed periodic fields. *Phys. Rev.*, 97:869–883, Feb 1955.

[24] JM Luttinger. Quantum theory of cyclotron resonance in semiconductors: General theory. *Physical review*, 102(4):1030, 1956.

[25] Lok C Lew Yan Voon and Morten Willatzen. *The kp method: electronic properties of semiconductors*. Springer Science & Business Media, 2009.

[26] Hyunsoo Kim, Kefeng Wang, Yasuyuki Nakajima, Rongwei Hu, Steven Ziemak, Paul Syers, Limin Wang, Halyna Hodovanets, Jonathan D Denlinger, Philip MR Brydon, et al. Beyond triplet: Unconventional superconductivity in a spin-3/2 topological semimetal. *Science advances*, 4(4):eaao4513, 2018.

[27] N. P. Butch, P. Syers, K. Kirshenbaum, A. P. Hope, and J. Paglione. Superconductivity in the topological semimetal yptbi. *Phys. Rev. B*, 84:220504, Dec 2011.

[28] Wang Yang, Tao Xiang, and Congjun Wu. Majorana surface modes of nodal topological pairings in spin-$\frac{3}{2}$ semimetals. *Phys. Rev. B*, 96:144514, Oct 2017.

[29] FF Tafti, Takenori Fujii, A Juneau-Fecteau, S René de Cotret, N Doiron-Leyraud, Atsushi Asamitsu, and Louis Taillefer. Superconductivity in the noncentrosymmetric half-heusler compound luptbi: A candidate for topological superconductivity. *Physical Review B*, 87(18):184504, 2013.

[30] Stanislav Chadov, Xiaoliang Qi, Jürgen Kübler, Gerhard H Fecher, Claudia Felser, and Shou Cheng Zhang. Tunable multifunctional topological insulators in ternary heusler compounds. *Nature materials*, 9(7):541–545, 2010.

[31] W. Al-Sawai, Hsin Lin, R. S. Markiewicz, L. A. Wray, Y. Xia, S.-Y. Xu, M. Z. Hasan, and A. Bansil. Topological electronic structure in half-heusler topological insulators. *Phys. Rev. B*, 82:125208, Sep 2010.

[32] Di Xiao, Yugui Yao, Wanxiang Feng, Jun Wen, Wenguang Zhu, Xing-Qiu Chen, G. Malcolm Stocks, and Zhenyu Zhang. Half-heusler compounds as a new class of three-dimensional topological insulators. *Phys. Rev. Lett.*, 105:096404, Aug 2010.

[33] PMR Brydon, DF Agterberg, Henri Menke, and C Timm. Bogoliubov fermi surfaces: General theory, magnetic order, and topology. *Physical Review B*, 98(22):224509, 2018.

[34] Aline Ramires, Daniel F. Agterberg, and Manfred Sigrist. Tailoring T_c by symmetry principles: The concept of superconducting fitness. *Phys. Rev. B*, 98:024501, Jul 2018.

[35] Yasuhiro Asano, Yakov V. Fominov, and Yukio Tanaka. Consequences of bulk odd-frequency superconducting states for the classification of cooper pairs. *Phys. Rev. B*, 90:094512, Sep 2014.

[36] F. S. Bergeret, A. F. Volkov, and K. B. Efetov. Long-range proximity effects in superconductor-ferromagnet structures. *Phys. Rev. Lett.*, 86:4096–4099, Apr 2001.

[37] Y. Tanaka and A. A. Golubov. Theory of the proximity effect in junctions with unconventional superconductors. *Phys. Rev. Lett.*, 98:037003, Jan 2007.

[38] Yasuhiro Asano and Yukio Tanaka. Majorana fermions and odd-frequency cooper pairs in a normal-metal nanowire proximity-coupled to a topological superconductor. *Phys. Rev. B*, 87:104513, Mar 2013.

[39] Y. Tanaka, Y. Asano, A. A. Golubov, and S. Kashiwaya. Anomalous features of the proximity effect in triplet superconductors. *Phys. Rev. B*, 72:140503, Oct 2005.

[40] Yasuhiro Asano, Alexander A. Golubov, Yakov V. Fominov, and Yukio Tanaka. Unconventional surface impedance of a normal-metal film covering a spin-triplet superconductor due to odd-frequency cooper pairs. *Phys. Rev. Lett.*, 107:087001, Aug 2011.

[41] Yasuhiro Asano and Akihiro Sasaki. Odd-frequency cooper pairs in two-band superconductors and their magnetic response. *Phys. Rev. B*, 92:224508, Dec 2015.

[42] Ya. V. Fominov, Y. Tanaka, Y. Asano, and M. Eschrig. Odd-frequency superconducting states with different types of meissner response: Problem of coexistence. *Phys. Rev. B*, 91:144514, Apr 2015.

[43] S. Mironov, A. Mel'nikov, and A. Buzdin. Vanishing meissner effect as a hallmark of in˘plane fulde-ferrell-larkin-ovchinnikov instability in superconductor˘ferromagnet layered systems. *Phys. Rev. Lett.*, 109:237002, Dec 2012.

[44] Shu-Ichiro Suzuki and Yasuhiro Asano. Paramagnetic instability of small topological superconductors. *Phys. Rev. B*, 89:184508, May 2014.

[45] Annica M. Black-Schaffer and Alexander V. Balatsky. Odd-frequency superconducting pairing in multiband superconductors. *Phys. Rev. B*, 88:104514, Sep 2013.

[46] Akihiro Sasaki, Satoshi Ikegaya, Tetsuro Habe, Alexander A. Golubov, and Yasuhiro Asano. Josephson effect in two-band superconductors. *Phys. Rev. B*, 101:184501, May 2020.

[47] Dakyeong Kim, Shingo Kobayashi, and Yasuhiro Asano. Josephson effect of superconductors with $j = \frac{3}{2}$ electrons. *Phys. Rev. B*, 103:184516, May 2021.

[48] P A Frigeri, D F Agterberg, and M Sigrist. Spin susceptibility in superconductors without inversion symmetry. *New Journal of Physics*, 6:115–115, sep 2004.

[49] P. A. Frigeri, D. F. Agterberg, A. Koga, and M. Sigrist. Superconductivity without inversion symmetry: Mnsi versus cept$_3$Si. *Phys. Rev. Lett.*, 92:097001, Mar 2004.

[50] B.D. Josephson. Possible new effects in superconductive tunnelling. *Physics Letters*, 1(7):251 – 253, 1962.

[51] Gerald. D Mahan. *Many-Particle Physics*. Plenum Press, New York, 1990.

[52] Vinay Ambegaokar and Alexis Baratoff. Tunneling between superconductors. *Physical Review Letters*, 10(11):486, 1963.

[53] PMR Brydon, Wei Chen, Yasuhiro Asano, and Dirk Manske. Charge and spin supercurrents in triplet superconductor-ferromagnet-singlet superconductor josephson junctions. *Physical Review B*, 88(5):054509, 2013.

[54] V. L. Berezinskii. New model of the anisotropic phase of superfluid he^3. *JETP Lett.*, 20:287, 1974.

[55] C. Caroli, P.G. De Gennes, and J. Matricon. Bound fermion states on a vortex line in a type ii superconductor. *Physics Letters*, 9(4):307–309, 1964.

[56] GE Volovik. Vortex motion in fermi superfluids and the callan-harvey. *JETP Lett*, 57(4), 1993.

[57] L. J. Buchholtz and G. Zwicknagl. Identification of p-wave superconductors. *Phys. Rev. B*, 23:5788–5796, Jun 1981.

[58] Jun'ichiro Hara and Katsuhiko Nagai. A Polar State in a Slab as a Soluble Model of p-Wave Fermi Superfluid in Finite Geometry. *Progress of Theoretical Physics*, 76(6):1237–1249, 12 1986.

[59] Igor Boettcher and Igor F. Herbut. Anisotropy induces non-fermi-liquid behavior and nematic magnetic order in three-dimensional luttinger semimetals. *Phys. Rev. B*, 95:075149, Feb 2017.